Rep. Prog. Phys. **62** (1999) 1333–1376. Printed in the UK PII: S0034-4885(99)88967-2

Archaeological dating using physical phenomena

M J Aitken†
Le Garret, Augerolles, Puy-de-Dôme, 63 930, France

Received 9 April 1999

Abstract

A review is given of the science-based techniques that have been used to establish archaeological chronologies from the million-year range down to the historical period. In addition to the discussion of nuclear, atomic and chemical methods indication is given of the way in which the Earth's magnetic field and perturbations of the Earth's orbital motions are useful in this.

† Emeritus Professor of Archaeometry, Oxford University.

0034-4885/99/091333+44$90.00

Contents

1. Introduction

Although it is no surprise that determination of the age of the Earth is based on physical phenomena it is less expected that this is also the case for the chronology of a substantial part of the archaeological record. Of course on Roman sites the layer-by-layer finds, particularly of coins with inscriptions, often permit dating by reference to the enduring writings of contemporary authors, for example Julius Caesar, and in any case such writings establish the basic chronology of the period. To some extent the same is true further back in time, notably by relating to the king-lists giving the reign durations of the Egyptian pharaohs; these lists extend back to the First Dynasty and the earliest pyramid at about 5000 years ago—though even this age is not science-independent since, because of missing sections of the lists, it is reliant on an astronomical calculation of the date of a recorded stellar event. Beyond 5000 years ago all was conjecture until the so-called 'radiocarbon revolution' in the early 1950s; from then on 'the deeper the older' was replaced by ages based on the laboratory-measured half-life of ^{14}C. These ages had a dramatic impact on prehistoric interpretation, emphatically marking the arrival of physics on the archaeological scene; in general terms radiocarbon ages indicated that the pace of human development had been substantially slower than previously assessed—a specific example being that earliest Jericho had been initiated some 10 000 years ago rather than the 6000 previously estimated.

The effective age-range of radiocarbon is about 40 000 years (except for special installations, see section 2.1.2); far beyond this a timescale for the early stages of hominid development several million years ago has been provided by the radioactive decay of ^{40}K and by the accumulation of tracks in certain minerals by fission fragments from uranium. Accumulation of effects due to natural nuclear radiation are also the basis of dating by means of luminescence and electron spin resonance; in the uranium-series method the basis of dating is the gradual return to radioactive equilibrium. These three methods have had wide applications including elucidation of the relationship of anatomically modern humans to Neanderthals. Besides radioactive decay and the cumulative effects of natural nuclear radiation there are a number of other chronological indicators—based on chemical change, on variations in the Earth's magnetic field, and on climatic changes associated with variations in the Earth's orbital motions. Some yield an absolute chronology, some are a means of transferring absolute chronology to other regions or to other sample types.

Besides the obvious requirement in a dating method that there is a measurable time-dependent quantity that forms the 'clock', it is necessary that there is an event that starts the clock and that this event, 'the event dated', is relatable to the archaeological event of interest. For some methods this is automatic, e.g. the thermoluminescence clock in pottery is set to zero by the firing of the kiln. In others the association may only be approximate, e.g. the radiocarbon clock in wood starts when the wood forms, not when the tree was felled nor at the time of human utilization; hence the emphasis on 'short-lived' samples such as grain and twigs.

There is a hierarchy of reasons for dating. At the top there are dates which have worldwide significance such as those concerned with hominid development. Then there are dates that establish the basic chronological framework of a region; a further reason is the need to date a site when there is doubt about its relationship to the region's chronological framework. In general terms, dating is necessary in order to have a proper understanding of human development, whether biological, cultural, or technological. An example is the impact on the diffusionist model of European prehistory—that civilization spread to barbaric western Europe from the Near East. The conflict of radiocarbon dates with those based on 'the further West, the later' led to the former being initially described as 'archaeologically unacceptable' but soon the

diffusionist model was abandoned in favour of a large degree of independent invention—western Europe was not so barbaric after all.

In what follows the physical bases of all currently used methods are indicated, with occasional outlines of an application; to illustrate the endeavours necessary to reach the stage of reliable dating somewhat fuller discussion is given of the two having widest applicability—radiocarbon and luminescence. In the interests of conciseness the references have been largely limited to papers that are either seminal or recent, however, fuller details of all aspects can be found in the books of Aitken (1985, 1990, 1998), Aitken *et al* (1993), Taylor (1987), Taylor and Aitken (1997) and Wintle (1996, 1997).

2. Radioactive decay

2.1. Radiocarbon

Radiocarbon dating is the dominant technique for organic samples of the last 40 000 years—wood (and charcoal), bone, peat, seeds, cloth, etc; it is important both in archaeology and in recent geology. It was developed by bringing together several diverse physical measurements, as will be seen from section 2.1.1.

2.1.1. Historical introduction. The weakly radioactive isotope ^{14}C is present in the atmosphere, in all living plants and animals, and in the dissolved carbonates of the ocean. This was established by W F Libby and his group at the University of Chicago in the late 1940s who were studying the effects of cosmic rays on the Earth's atmosphere and it led to the idea of age determination using radiocarbon (see Libby 1965); Libby subsequently received a Nobel prize for this work. The presence of ^{14}C in living matter was predicted from a high-altitude balloon-flight measurement of the neutron flux produced by cosmic rays together with laboratory measurement of thermal neutron cross sections. The predominant way in which neutrons interacted with the atmosphere was found to be with the principal isotope of nitrogen according to

$$^{14}\mathrm{N} + \mathrm{n} \rightarrow {}^{14}\mathrm{C} + {}^{1}\mathrm{H}. \qquad (2a)$$

Because this is the predominant interaction the global ^{14}C production rate is nearly equal to the global neutron production rate; from balloon measurements that the average neutron flux is about 2 s^{-1} cm^{-2} this yields a global ^{14}C production rate of close to 7.5 kg per year. For the equilibrium situation this is also the global decay rate.

As illustrated in figure 1 the ^{14}C oxidizes to heavy carbon dioxide and mixes in with the non-radioactive carbon dioxide of the atmosphere, thence into the organic constituents of all living matter and also into the carbonate of the oceans; this carbon exchange reservoir was estimated to contain about 40×10^{12} tonnes of stable carbon (^{12}C) and combined with the above decay rate the predicted specific radioactivity was close to 15 decays min^{-1} (250 Bq) per gram of natural carbon. Each decay is accompanied by a beta particle and so this is also the specific beta activity.

Experimental confirmation was sought by measurement of samples of the methane given off by City of Baltimore sewage. The sample was converted into carbon black and painted on the inner wall of a modified Geiger counter; the sample needed to be inside the counter because besides the emission rate being low, the beta particles (maximum energy 0.16 MeV) are weak in terms of penetrating power, the flux being halved by a 10 μm thickness of aluminium. There was gratifying agreement with prediction and measurements were then extended to growing wood from different parts of the world and of recently formed seashell; the same specific

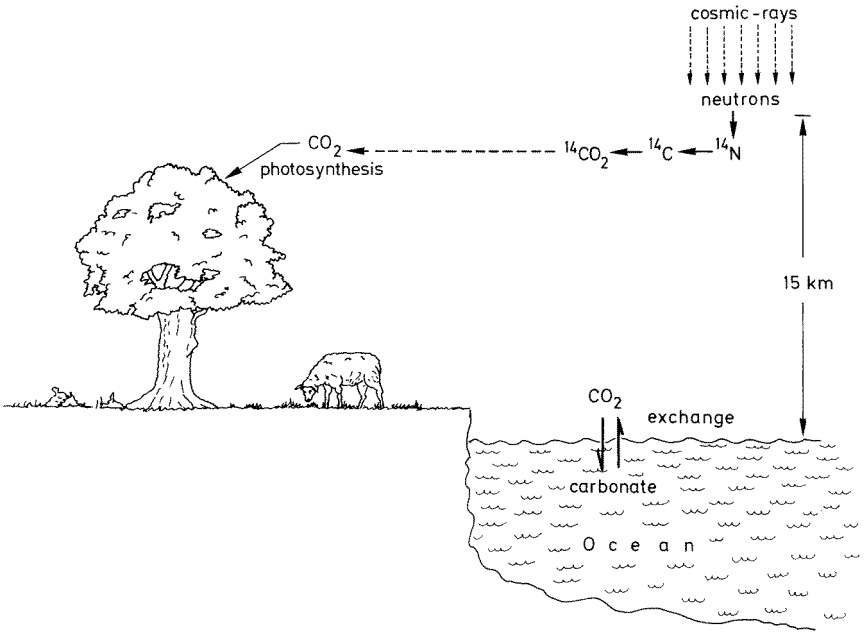

Figure 1. After formation high up in the atmosphere, with maximum production at about 15 km, ^{14}C is oxidized to 'heavy' carbon dioxide whence it rapidly mixes in with the non-radioactive carbon dioxide of the atmosphere. It then enters other parts of the carbon-exchange reservoir as illustrated (from Aitken 1990).

activity was found, giving evidence of good mixing throughout the carbon exchange reservoir (Libby *et al* 1949).

When wood cellulose or shells are formed the carbon atoms are fixed and so are cut off from the exchange reservoir; hence radioactive decay is no longer balanced by neutron-induced production and the specific activity should decrease according to the 5730-year half-life. Confirmation was sought by measurement of wood from the tombs of the Egyptian kings Zoser and Sneferu; from historical records it was known that these kings died within 75 years of 2550 BC (4500 years ago) and so it was with considerable excitement that the beta activity was found to be a little over half the value for recently grown wood. Further results (see figure 2) confirmed the validity, within the limits of error, of reversing the process and obtaining the age of a sample by means of its beta activity — the start, for prehistoric archaeology, of the radiocarbon revolution (section 1).

2.1.2. Measurement. The Geiger counter technique was soon superseded by use of a gas proportional counter because of its greater efficiency and lower vulnerability to external contamination. The sample is converted into carbon dioxide, methane, or acetylene and then used as the counting gas. Heavy steel and/or lead shielding, several tons of it, is the primary protection against the beta counts being swamped by cosmic-ray background; in addition there is a surrounding ring of anticoincidence detectors. In a typical installation the count-rate from a few grams of modern carbon is about 20 min^{-1}; with good shielding the background can be as low as about one count min^{-1}. Of course the count-rate for old samples is much lower and so counting times of several days may be necessary. When plenty of sample material is available it is advantageous to obtain higher count-rates by using a liquid scintillation counter.

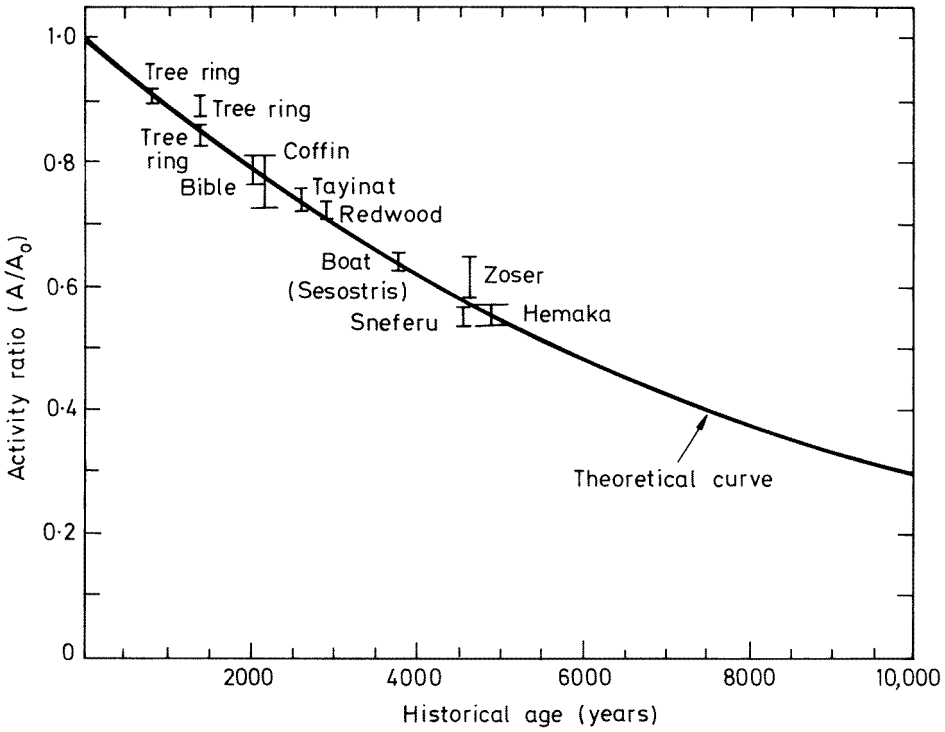

Figure 2. The first comprehensive test, using dated tree-rings and wood from Egyptian pyramids (redrawn from Arnold and Libby 1949). The vertical scale shows the ratio of the radioactivity of the ancient sample to that from a modern one. The theoretical curve is based on the then evaluated half-life of 5570 years (from Aitken 1990).

For this the carbon from the sample is converted to benzene and used as the solvent for a scintillator; the containing vial is viewed by two photomultipliers in coincidence mode.

However good the experimental quality of a laboratory the ultimate limitation in age range is around 40 000 years—because the sample-plus-background count-rate then becomes indistinguishable from the background count-rate. However, by employing thermal diffusion columns to obtain isotopic enrichment before measurement several laboratories have achieved five-fold enrichment of ^{14}C relative to ^{12}C thereby pushing back the limiting age to around 70 000 years. For this, and indeed in any case, absence of contamination is crucial, particularly contamination by modern carbon: the presence of 1% in a 34 000-year-old sample will cause the age to be overestimated by 4000 years; for an infinitely old sample the apparent age will be 38 000 years. It is not only a matter of avoiding contamination during sample preparation; sample integrity is also of critical importance—as illustrated in figure 3.

During the 1980s several laboratories initiated the use of accelerator mass spectrometry (AMS) using a tandem electrostatic generator for acceleration of the ions; higher voltages than those used in ordinary mass spectrometry are needed in order that various nuclear physics techniques can be used for particle detection and discrimination against unwanted ions. The basic advantage of AMS is that it is essentially an 'atom counting' technique; this is highly advantageous compared with beta counting because only 1% of the ^{14}C atoms emit a beta particle in about 80 years. Whereas with AMS, depending of course on the age of the sample, a statistical precision of $\pm 0.5\%$ can be obtained in a few hours using only a few milligrams

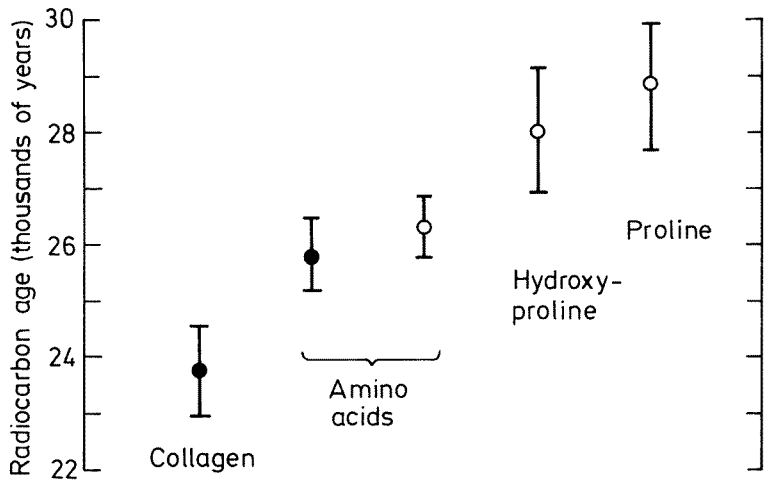

Figure 3. Radiocarbon ages for different constituents extracted from a rhinoceros bone. The older ages obtained for the proline and hydroxyproline, which are amino acids generally specific to bone, suggest intrusive contamination in the other constituents. Open symbols indicate AMS measurement and closed symbols conventional beta decay counting (from Aitken 1990).

of total carbon, with beta counting the time necessary to obtain the same precision is a matter of days, even though several grams are used. Not only does the lower weight requirement give access to a new range of samples, e.g. single seeds, but it also allows determinations to be made on separate chemical components of a sample, some of which may be more reliable than others—particularly in the case of bone, as already illustrated in figure 3.

Evaluation of a date is based on the ratio between the sample activity (or the $^{14}C/^{12}C$ ratio in the case of AMS) and a value representing present-day activity. To avoid error due to drift in equipment efficiency it is necessary to measure some form of standard immediately after the sample being dated. It is not satisfactory to use a recently grown sample for this because of human disturbance to the ^{14}C activity of the atmosphere; one option is to use a sample which acquired its ^{14}C in the nineteenth century and calculate the 'modern' value—in practice the value for AD 1950 is used (see section 2.4). One form of human disturbance is due to the burning of fossil fuel; this releases into the atmosphere vast quantities of carbon dioxide from which the ^{14}C has long since decayed — because coal and oil were removed from the exchange reservoir millions of years ago. This 'old' carbon significantly dilutes the ^{14}C in the atmosphere and the ^{14}C activity found in wood grown in AD 1950 (prior to nuclear weapons testing) is lower by about 3% than would have otherwise been the case. The other form of disturbance has been the atmospheric testing of nuclear weapons; neutrons released in fission and fusion explosions cause the formation of ^{14}C and in the mid-1970s the atmospheric activity was approximately double the level in the pre-testing era. In what follows it is convenient to use the 'activity of recently grown material' to denote the activity that such material would have had in the absence of these disturbances.

Allowance for isotopic fractionation. Because of isotopic fractionation not all types of living material have the same activity; for instance, in the process of photosynthesis by which plants obtain carbon from the atmosphere ^{14}C is not taken up so readily as ^{12}C, to the extent that the activity in plants can be as much as 5% lower than the carbon dioxide of the atmosphere

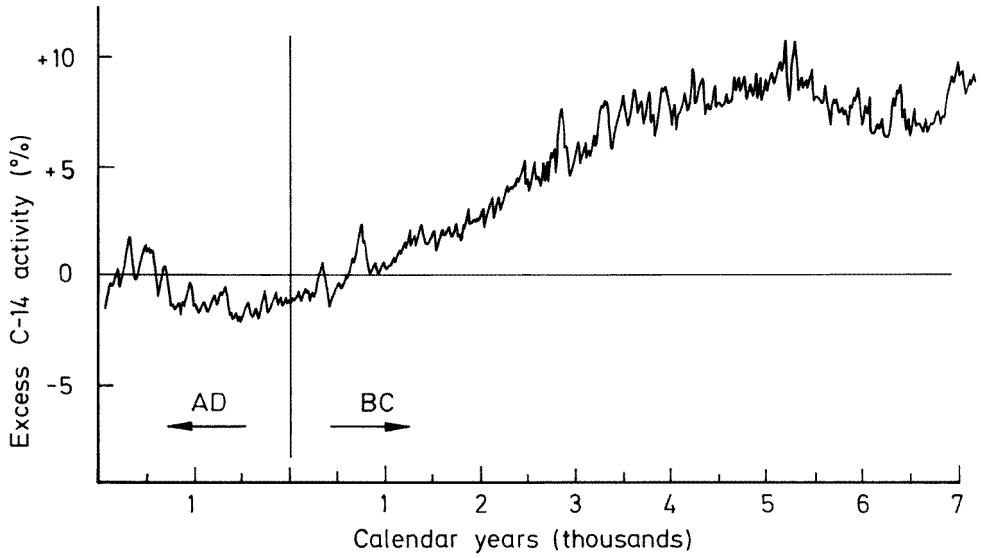

Figure 4. Radiocarbon activity in the atmosphere relative to the value for the late nineteenth century (redrawn from Stuiver *et al* 1986). The data have been derived from measurements on dendrochronologically dated wood. An excess of 1% corresponds to an age underestimation of 83 years if correction is not made (from Aitken 1990).

(equivalent to an apparent age excess of about 400 years). There are small variations from species to species in the degree of fractionation and allowance is made by mass spectrometric measurement of the degree of fractionation shown by the stable isotope ^{13}C which is present to about 1% of the level of ^{12}C; because the percentage depletion for an isotope is proportional to the difference in atomic mass, the depletion for ^{14}C is obtained by doubling that found for ^{13}C.

Allowance for residence time (reservoir effect). Carbon atoms spend only a few tens of years in the atmosphere and surface ocean before reaching the deep ocean but on average carbon atoms spend the order of a thousand years there before returning to the atmosphere by the exchange reaction at the surface between carbonate and carbon dioxide. Consequently there is a deficiency of ^{14}C in carbonate of the deep ocean because loss by radioactive decay is occurring without full replenishment by fresh production. The surface is intermediate between deep ocean and atmosphere since the carbon in it is a mixture of 'reinvigorated' carbon from the atmosphere and 'old' carbon from the deep ocean; the apparent age is usually of the order of 400 years and this needs to be subtracted from the age evaluated for a marine sample—though this will be an underestimate for samples which grew in regions of deep-water upwelling.

2.1.3. Distortions of the radiocarbon timescale. As measurement techniques improved it became evident that the ages of wood from early Egyptian tombs were being underestimated and this tendency was confirmed by measurements on dendrochronologically-dated wood (see section 6.1) that were made from the late 1950s onward (see Suess 1986). Underestimation of age corresponds to the sample having had a higher initial activity than recently grown material; the implied excess activity in the atmosphere is illustrated in figure 4. Further back in time, data have been obtained from paired ^{14}C and uranium-series measurements on corals (Bard *et al* 1990) and from ^{14}C measurements on organic matter contained in annually laminated

sediments ('varves') in lakes and on the sea bed—the dating being essentially by counting. Measurements on two sets of such sediments now extend back to around 40 000 years ago (Kitagawa and van der Plicht 1998; Voelker *et al* 1998); these indicate that for a range of intermediate millennia the ^{14}C excess reached a maximum of nearly 40%, corresponding to an age underestimation of about 3000 years.

Long-term excess of ^{14}C indicates either that the cosmic-ray intensity was higher in the past than at present or that the exchange reservoir was smaller. Higher intensity is consistent with palaeomagnetic indications that the Earth's magnetic field has been weaker in the past than at present thus reducing deflection of cosmic rays away from the Earth; the above data correlate well with calculation of the excess based on the palaeomagnetic data, though not ruling out subsidiary reservoir effects due to changing oceanic circulation (e.g., Laj *et al* 1996, Bard 1998). The short-term 'wiggles' of figure 4 are mostly attributable to modulation of the cosmic-ray flux by magnetic effects of the solar wind, with likely contributions from oceanic effects also (Stuiver and Braziunas 1993, Bard *et al* 1997); another nuclide generated in the atmosphere by cosmic rays, ^{10}Be, is useful in this context. This, together with two other cosmogenic nuclides, ^{26}Al and ^{36}Cl, is also of interest for dating on a longer timescale than ^{14}C; however the latter is unique in the combination of properties, particularly its uniform distribution throughout the biosphere, that make it suitable for archaeological application.

2.1.4. Conversion to calendar dates. Though interesting from the geochemical and geophysical point of view the foregoing section hardly seems to justify the reputation of radiocarbon as an accurate and reliable method of age determination. That this reputation is well-deserved is due to the highly refined calibration data by which radiocarbon ages are converted to calendar dates. Figure 4 is based on the detailed measurements reported in 1986 (Stuiver and Kra); radiocarbon dates, mostly with an accuracy of ± 20 years, were obtained for successive 10- or 20-year packets of known-age tree-rings from several sequences—some from high altitude trees, mainly Douglas fir and sequoia, which had grown on the US Pacific coast, and some from trees, mainly oak, that had grown in lowland Europe. There was excellent agreement between data obtained for contemporary trees from Europe and the US, as also between duplicate results in two independent laboratories—at Belfast using a liquid scintillator and at Seattle using a gas proportional counter. Refinement and extension of calibration data continues (e.g. Stuiver *et al* 1998).

A more complex aspect of calibration is the increased ambiguity in interpretation that results from the short-term wiggles; these are confirmed as real by inter-laboratory and inter-sequence comparison. A rapid decrease in activity with decreasing calendar age can result in the radiocarbon age for a sample being greater than that for an older sample, i.e. the radiocarbon clock goes backwards; where the decrease in ^{14}C activity is prolonged but slower a 'plateau' can result—a calendar period when there is little change in radiocarbon age. A notable example is provided by the activity decrease that occurs between near 800 and 400 BC; another is the decrease from AD 1660 to 1950—with the result that radiocarbon dating is not utilizable for recent samples. On the other hand, in the context of dendrochronology (section 6.1), 'wiggle matching' can be highly advantageous; by matching the irregularities in the ^{14}C activities in a sequence of tree-rings unanchored in time, to corresponding irregularities in the master calibration a highly accurate age for the sequence can be obtained.

The complexity introduced by wiggles is illustrated in figure 5, which shows the calibration of the radiocarbon age obtained for the Shroud of Turin. At the 95% level of confidence there are two possible calendar dates and the question arises as to what are the relative probabilities of these. An approach to such questions is illustrated in figure 6; it will be seen that this contains more information than is given by the central date and confidence level spans.

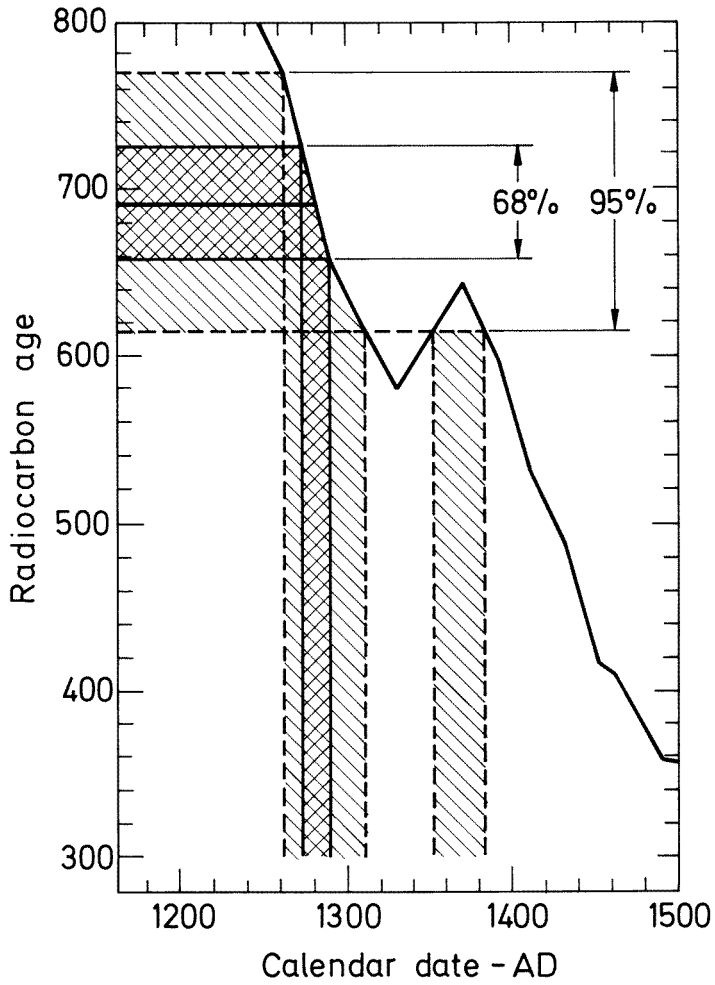

Figure 5. The Shroud of Turin. Calibration of the radiocarbon age of 691 (±31) years as derived from measurements by three AMS laboratories on linen threads (see Damon *et al* 1989). After allowance for a small uncertainty in the calibration curve (Stuiver and Pearson 1986) the calendar date span corresponding to the 68% level of confidence is AD 1275–1290; corresponding to the 95% level of confidence there are two possible spans: AD 1260–1310 and AD 1355–1385 (from Aitken 1990).

Nomenclature. Raw or 'conventional' radiocarbon ages are specified as so many years BP (before present). Such ages are calculated on the basis of the original Libby half-life of 5568 years and the ratio between the sample's activity, A, and that of a modern standard, A_{m}, measured in the same installation at about the same time; it is common practice to use a modern standard of the same material as the sample being measured. The age in conventional radiocarbon years BP is given by

$$\text{Age} = 8033 \ln\{A/A_{\mathrm{m}}\}. \qquad (2b)$$

The numerical factor is the mean life corresponding to a half-life of 5568 years rather than the revised half-life of 5730 years; use of the latter increases the age obtained by some 3%—a correction that is subsumed in calibration.

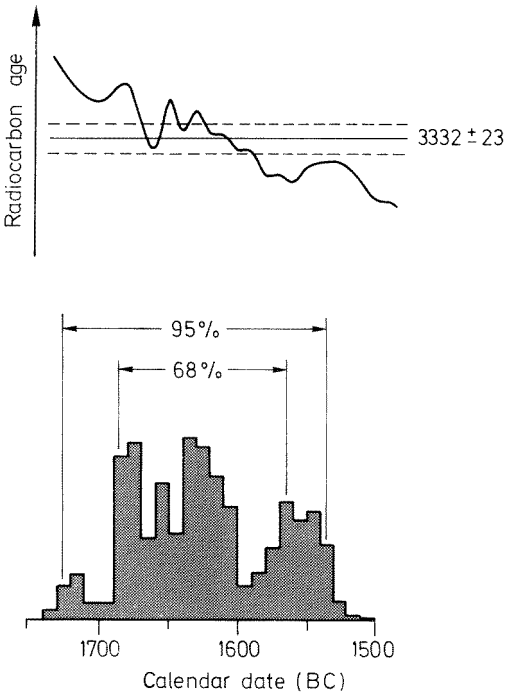

Figure 6. The Bronze Age eruption of Thera (section 6.4). Probability distribution (Robinson 1989 personal communication) for the calendar date corresponding to a radiocarbon age of 3332 (±23) years obtained by beta counting for short-lived samples from the associated destruction layer; the average radiocarbon age of 3325 (±30) years obtained by AMS from single seeds and grain etc (Houseley *et al* 1990) is in good agreement. Contrary to the situation in figure 5 the calibration curve (Stuiver and Becker 1986) is rather flat here and consequently the calendar date spans for a given confidence level are substantially wider than the corresponding radiocarbon age error limits (from Aitken 1990).

In order to avoid needing to know the date of measurement, 'modern' and 'present' are defined as AD 1950. Alternatively 'BP' can be regarded as meaning 'before physics'—AD 1950 being the year in which radiocarbon dates began to be published. When calibration has been performed the age is quoted as so many years 'cal BP'; alternatively it can be quoted as a calendar date, AD or BC, optionally inserting 'cal'.

2.2. Potassium–argon

Use for the dating of early hominids began in 1959 with application in the Olduvai Gorge in East Africa. It is widely used geologically to date volcanic products and in fact hominid application is indirect, it is volcanic levels that are dated, e.g. the lava flows above and below the hominid remains. Archaeological application, and the technique itself, has been reviewed by Walter (1997).

2.2.1. Outline. In naturally occurring potassium there is a weakly radioactive isotope, ^{40}K, having a natural atomic abundance of 117 ppm and a half-life of 1.25×10^9 years. About 90% of the decays are by beta emission to ^{40}Ca and 10% by electron capture to ^{40}Ar. It is the accumulation of this gas within potassium-bearing minerals that is the basis of dating; this is on the assumption that while molten in the volcanic magma there was no retention of argon and that subsequent to cooling the retention was total.

Measurement of the atomic contents, ^{40}Ar and ^{40}K, in a sample allows evaluation of T, the time elapsed since cooling, according to the equation

$$^{40}\mathrm{Ar}/^{40}\mathrm{K} = 0.1048\{\exp(T/\tau) - 1\} \qquad (2c)$$

where the numerical factor is the fraction of the ^{40}K decays yielding argon, and τ the mean life of ^{40}K. In this equation it is of course the amount of radiogenic argon that is relevant rather

than any atmospheric argon (present at a level of 1%) that may be in the sample. Distinguishing these two is one necessity in measurement; another is in determining whether or not there has been any leakage of argon since cooling.

The long half-life of ^{40}K more than encompasses the range required for hominid application; for samples at the young end of the age-range accumulation of argon is only slight but nevertheless with technological advance in measurement younger and younger ages are being obtained—the order of 10 000 years in good circumstances with minerals of high potassium content such as sanidine.

2.2.2. Measurement. Traditionally, the potassium content is measured by atomic absorption spectrometry, or some comparable technique, and the argon by mass spectrometry after release by fusion. Contamination by atmospheric ^{40}Ar is assessed by measurement of ^{36}Ar, also present in the atmosphere, the atmospheric ratio being known. Although of comparable sensitivity to the accelerator-type mass spectrometer used for radiocarbon dating the high-energy input is not necessary in this case.

The argon–argon method. The potassium content can also be assessed by means of irradiation with high energy neutrons in a nuclear reactor. This converts some of the potassium into ^{39}Ar and this is measured in the mass spectrometer at the same time as the ^{40}Ar; the age is then determined from the ratio between the two. An immediate advantage is that both isotopes are obtained from the same part of the sample thus avoiding any problem due to heterogeneity.

Another advantage is that the argon can be released by stepwise heating to successively increasing temperatures and an age evaluated for the gas released at each step. For a well-behaved sample the age stays the same for all steps of gas release and a plateau is obtained; on the other hand if, due to alteration associated with weathering, some of the less firmly held argon has been lost during burial, the age obtained for gas released during the early steps will be lower than that for later steps.

By using a high-power laser for release of argon, determinations can be made on single grains, stepwise heating still being possible. Such single crystal laser fusion (SCLF) has the very strong advantage that intrusive grains from older or younger strata can be detected and ignored; it also permits selection of the most advantageous minerals without the need for mineral separation.

2.3. Uranium-series

The principal radioisotope involved, ^{230}Th, has a half-life of 75 400 years—an order of magnitude greater than that of ^{14}C and its dating capability reaches back to 500 000 years thus covering important developments in hominid evolution. It extends into quite recent times, even to a 1000 years ago; thus it overlaps radiocarbon, but the latter encompasses a wider range of archaeologically relevant sample types and hence remains dominant within its 40 000-year range. Among reviews of the technique and its archaeological applications are those by Schwarcz (1980, 1992, 1997).

2.3.1. Basis The chain of daughter radioisotopes that follow the decay of ^{238}U is shown in figure 7; ^{238}U is the principal component of natural uranium, with an atomic abundance of 99.3%. The essential basis of dating is the re-growth of the daughter ^{230}Th into radioactive equilibrium after an event that has placed ^{238}U and ^{234}U in the sample unaccompanied by attendant daughters; this is the event that is dated. In circumstances for which it is valid to

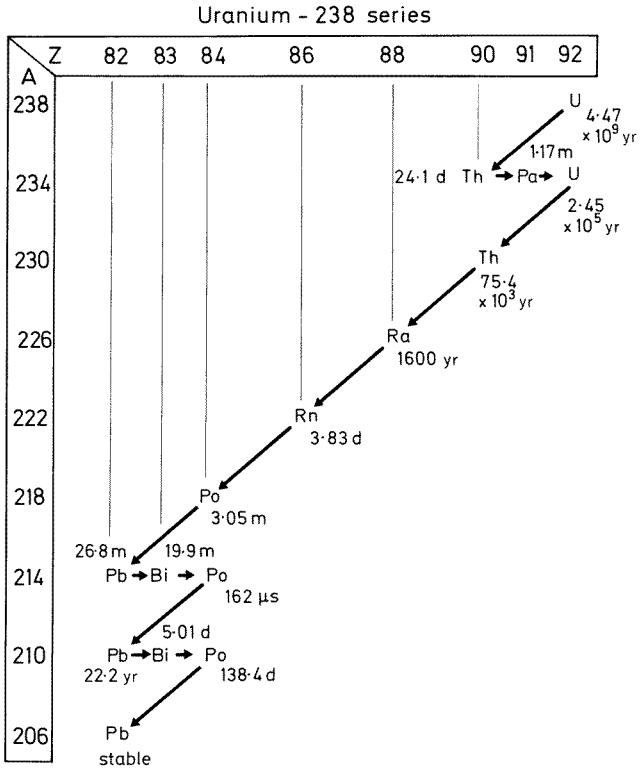

Figure 7. The major uranium decay chain. A long arrow indicates emission of an alpha particle and a short one emission of a beta particle. Branching less than 1% is not shown (from Aitken 1985).

assume that the initial activities (disintegrations per unit time) of ^{238}U and ^{234}U were equal, the age, T, can be derived from the equation

$$^{230}\text{Th} = {}^{238}\text{U}\{1 - \exp(-T/\tau)\} \tag{2d}$$

where ^{230}Th and ^{238}U represent the measured activities, and τ is the mean life of ^{230}Th.

It should be noted that τ determines the rate of grow-in of ^{230}Th as well as its rate of decay. This may be seen by solving the differential equation relating the rate of growth of a daughter to the quantity of daughter atoms present at time t:

$$\mathrm{d}N/\mathrm{d}t = A - \lambda N \tag{2e}$$

where N is the quantity of daughter atoms, λ is the daughter's probabilty of decay per unit time ($\lambda = 1/\tau$), and A is the activity of the long-lived parent.

Stalagmitic calcite, such as formed in limestone caves, is one of the principal archaeological materials concerned. Stalagmites and stalactites are formed from carbonate in ground water percolating into such caves and in this water uranium is usually present (albeit at trace impurity levels) but not thorium, because of its low solubility. Uranium is incorporated in the calcite crystals forming the stalagmites and stalactites; subsequently ^{230}Th grows-in until its activity is equal to that of the parent ^{238}U. Crystallization is the event dated and the time that has elapsed since this is determined using equation (2*d*).

In natural uranium there is also a small amount of ^{235}U (atomic abundance: 0.72%) and within its chain of daughters there is one long-lived radioisotope, ^{231}Pa, with a half-life of

34 800 years. For samples that are rich in uranium this too can be used for dating, in the range 5000–150 000 years, and in conjunction with ^{230}Th it is useful in establishing whether or not the sample fulfils the requirement of being a 'closed system'—see below.

2.3.2. Measurement. For dating by ^{230}Th, in addition to the activity of that radioisotope the activities of ^{234}U and ^{238}U are required. The activity of ^{234}U only is not enough since it is not necessarily in radioactive equilibrium with ^{238}U at time zero—in groundwater the ^{234}U activity is typically higher than the ^{238}U activity by around 10%; note from figure 7 that the half-life of ^{234}U is 245 000 years, hence it moves only gradually towards equilibrium with ^{238}U. Traditionally, these three activities are measured by alpha spectrometry; this follows the addition of tracers to the sample, chemical extraction, and deposition in a thin layer. Each of the three radioisotopes and the tracers has a characteristic energy of alpha emission; additionally it is advantageous to check for detrital contamination as indicated by the presence of ^{232}Th, a very long-lived alpha emitter; the ingress of ^{232}Th is likely to have been accompanied by ^{230}Th thus upsetting the necessary condition of zero activity of ^{230}Th at time zero.

As with radiocarbon more rapid determination and much better accuracy can be obtained by using mass spectrometry, enabling the age range to be from a few hundred years to half a million; the minimum sample size is also reduced. The technique, thermal ionization mass spectrometry (TIMS), does not require a nuclear accelerator but is costly nevertheless.

For determinations on precious hominid remains it is advantageous to use gamma spectrometry because this can be used non-destructively, though the accuracy attainable is severely impaired. Skulls and other human bones have been dated in this way (e.g. Yokoyama and Nguyen 1981, Berzero *et al* 1997, Simpson and Grün 1998, Schwarcz *et al* 1998).

2.3.3. Sample types and sample integrity. In caves having had human occupation stalagmitic calcite has proved reliable as long as care is taken to reject samples showing evidence of recrystallization — which of course starts the clock again; samples with detrital contamination, evidenced by the presence of ^{232}Th, must also be avoided. Dating of calcite incrustations on skeletal fragments is possible as long as TIMS is available to cope with the small sample size.

There are two problems with bone and carefully devised stratagems are necessary to avoid pitfalls. First, the uranium content of living bone is insignificant and it is only during burial that appreciable concentrations (1–1000 ppm) are acquired. If it is assumed that the uranium is taken up from ground water rapidly after burial, then dates may be evaluated on the same basis as for stalagmitic calcite; as with the latter, thorium is not available on account of insolubility. On the other hand, if the take-up was gradual then there will be a deficit in the amount of ^{230}Th that has grown-in. Secondly, because of its porous structure bone is prone to 'open system' effects and degradation; if some of the uranium has been leached out from the bone during burial, but the ^{230}Th has remained because of its lower solubility, then the measured ratio will be erroneously high. As mentioned above, lack of concordance with the age derived from ^{231}Pa is one indication that this has happened; there are other more subtle ones. Tooth dentine suffers from the same uncertainties as bone and to some extent tooth enamel also does. The topic of uranium uptake will be discussed further in the context of ESR dating (section 3.2).

Mollusc shells, particularly of the aragonitic variety, have not lived up to expectations of reliability. On the other hand, the eggshells of large flightless birds (ratites, e.g. ostriches) are resistant to leaching on account of their dense calcite matrix and are reliable (see section 4.1); of course use of TIMS is essential on account of the small amount of material available. Coral is material *par excellence* and although not of direct archaeological relevance it has been highly important in the calibration of the radiocarbon timescale.

3. Cumulative effects of nuclear radiation

The preceding techniques are nuclear in the strict sense of the word: the essence of the dating clock is the build-up of a daughter product, as with potassium–argon and uranium-series, or the gradual disappearance of a radioactive isotope, as with radiocarbon. Being based on the immutable rate of radioactive decay they are less prone to external circumstances than the cumulative nuclear techniques that now follow—though as we have seen in practice the strictly nuclear techniques are far from immune, albeit for secondary reasons.

3.1. Luminescence

3.1.1. Outline. Unlike the preceding techniques luminescence dating is remarkable in utilizing a phenomena of which variants can be seen with the naked eye. Bioluminescence is the commonest of these, and there is reference to fireflies in Chinese literature as early as three millennia ago; glow worms and the phosphorescence of sea water are other manifestations as well as the luminous bacteria which feed on decaying flesh. More relevant to luminescence dating is the so-called 'cold light' emitted by some gems and stones—'cold' referring to the occurrence of emission at a temperature lower than that needed for red-hot glow.

There are recorded observations of cold light from inorganic substances over the last two thousand years but it is from the mid-seventeenth century onwards that serious scientific studies were made. It was the advent, near the middle of the twentieth century, of the photomultiplier as a very sensitive detector of light that led to a multiplicity of luminescence applications: investigation of crystal structure and defects; meteorite and lunar studies; dosimetry of x-rays and nuclear radiation; dating of archaeological pottery, of burnt flint, of volcanic products, of stalagmitic calcite, and of geological sediment. So luminescence dating was not 'out of the blue' like radiocarbon but had a substantial pedigree.

Mechanism. There are two variants of luminescence dating: thermoluminescence (TL) and optically stimulated luminescence (OSL), the latter also being referred to as optical dating. For both variants, the latent dating information is carried in the form of trapped electrons; these are electrons which have been ionized by nuclear radiation and which have diffused into the vicinity of a defect in the lattice that is attractive to electrons, such as a negative-ion vacancy, and have become trapped there. The nuclear radiation is from radioelements in the sample and in its surroundings; there is also a small contribution from cosmic rays. The more prolonged the exposure to ionizing radiation the greater the number of trapped electrons, which hence increases with the years that have elapsed since the last event at which the traps were emptied. This setting of the clock to zero is the event dated and it can be due to the agency of heat, as with pottery, or of light, as with geological sediment.

A measure of the number of trapped electrons is obtained by stimulation—by heat in the case of TL and by light in the case of OSL. In either case stimulation causes the eviction of electrons from their traps whereupon they diffuse around the crystal until some form of recombination centre is found, such as a defect activated by being charged with a hole. The time spent in diffusion is very short and recombination can be regarded as instantaneous. In the case of a luminescence centre there is emission of light, the colour being characteristic of the type of centre. Figure 8 gives an indication of the overall mechanism; it is an over-simplified representation of reality but forms a useful basis for discussion.

It is presumed that there is no shortage of activated luminescence centres and also that the radiation flux is not sufficient to cause any significant increase in the number of centres over the age span of the sample. An alternative to the picture given is to consider the process to be

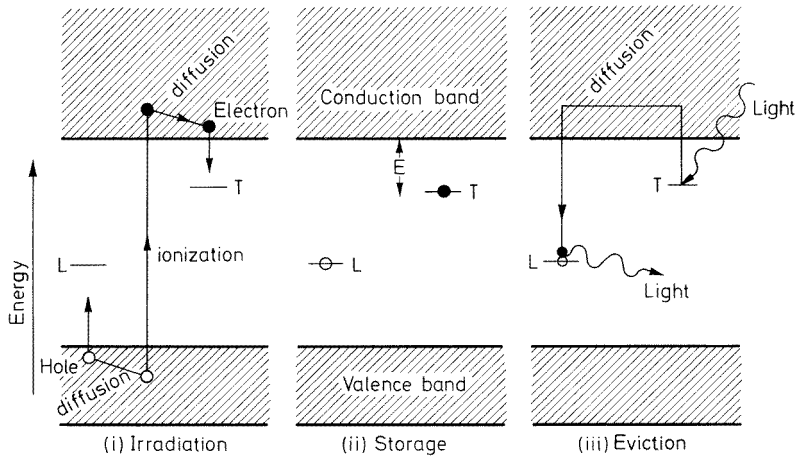

Figure 8. Energy-level representation of the OSL process. (i) Ionization due to exposure of the crystal to the flux of nuclear radiation, with trapping of electrons and holes at defects, T and L respectively. (ii) Storage during antiquity; in order that leakage is negligible the lifetime of the electrons in the traps needs to be much longer than the age span of the sample. This lifetime is determined by the depth E of the trap below the conduction band and for dating purposes we are interested in those deep enough ($\sim$1.6 eV or more) for the lifetime to be at least several million years. (iii) By shining light of appropriate wavelength onto the sample, electrons are evicted from traps and some of these reach luminescence centres; if so, light (i.e. OSL) is emitted in the process of combining into these centres. Alternatively, the electrons may recombine at non-luminescence centres ('killer' centres), be recaptured by a trap of the same type, or be captured by another type of trap. The TL process is similar except that stimulation is by heat: a temperature is reached at which the thermal vibrations of the crystal lattice are sufficient to cause eviction, the deeper the trap the higher the temperature necessary (from Aitken 1998).

dominated by trapped holes; however, although this may represent reality in some cases it is irrelevant to the discussion of most phenomenon and it is convenient to use a description based on trapped electrons. A similar description is relevant to dating by electron spin resonance (ESR) except that there is then no eviction. The three techniques are sometimes grouped together under the heading of trapped electron dating (TED) or of trapped charge dating (TCD).

Evaluation of age. The basis is summarized in figure 9. The 'natural' signal—that resulting from the natural irradiation during burial—is compared with signals, from the sample, resulting from known doses of nuclear radiation; these are administered by a calibrated radioisotope source. This procedure allows evaluation of the *paleodose*—the laboratory dose of nuclear radiation needed to induce 'artificial' luminescence equal to the natural signal. In principle the age is then given by

$$T = \frac{\text{Paleodose}}{\text{Dose-rate}}. \tag{3a}$$

The *dose-rate* represents the rate at which energy is absorbed from the flux of nuclear radiation; it is evaluated by assessment of the radioactivity of the sample and its surrounding burial material; this is carried out both in the laboratory and in the field.

Application. Currently, together with flint and calcite, the minerals of dominant interest archaeologically are quartz and feldspar, whether from pottery (to which mineral grains are

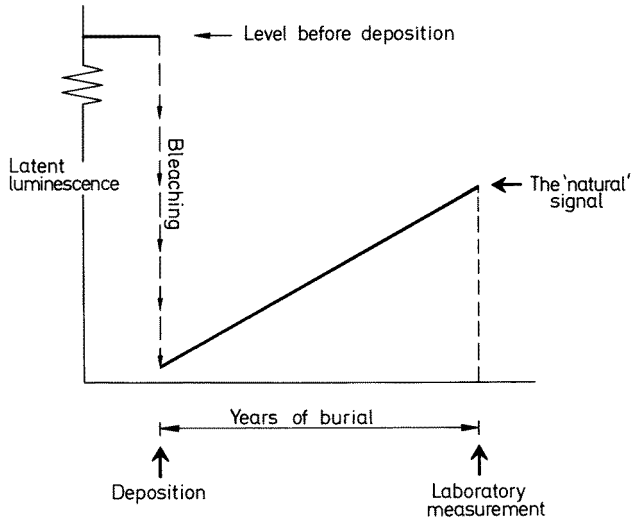

Figure 9. The event dated, whether in thermoluminescence dating or in optical dating, is the setting to zero, or near zero, of the latent luminescence acquired at some time in the past. With sediment this zeroing occurs through exposure to daylight ('bleaching') during erosion, transport, and deposition, whereas with fired materials, it is through heating. Subsequently the latent signal builds up again through exposure to the weak natural flux of nuclear radiation. For OSL the dating signal is obtained by exposure of the grains from the sample to a beam of light; for TL it is obtained by heating (from Aitken 1998).

added as temper), from sediment, or from volcanic products. The age range covered by the various types of sample and technique is remarkable—from a few tens of years to around half a million. The limitation with quartz and flint is usually due to the onset of saturation—when all traps have become occupied; with feldspar it is more likely to be due to inadequate electron retention in the traps.

The wide age range is matched by a multiplicity of applications. The initial impact of TL was in the authenticity testing of art ceramics, a revolutionary impact comparable with that of radiocarbon in archaeology. In parallel there was increasing use of TL for radiation dosimetry in health physics—radiotherapy, and radiation protection in general, and retrospective dosimetry (Bailiff 1997). Because of its poorer precision than radiocarbon its use for dating archaeological sites by application to pottery has been limited, though it has the advantage that its samples are directly linked to archaeological chronology and uncertainties of association are avoided. Of more importance has been the use of TL from burnt flint in reaching back well beyond the 40 000-year limit of radiocarbon; stalagmitic calcite also has a role in this context though uranium series is usually to be preferred for that material. By dating flints associated with skeletons found in Palaeolithic cave sites in western Asia it was established that anatomically modern humans were present there at around 100 000 years ago (Mercier *et al* 1995); this gave strong support to the view that these hominids developed in parallel with Neanderthals rather than being descendants, the latter relationship having been the traditional assumption. In Earth-science studies it is useful in such widely divergent contexts as sand dunes and other features of climatic aridity, raised shoreline and fluvial deposits, and Arctic glacial-marine sediments. Above all, it is applicable to the windblown loess deposits that cover vast areas of the Earth's surface and in which many Palaeolithic sites are buried.

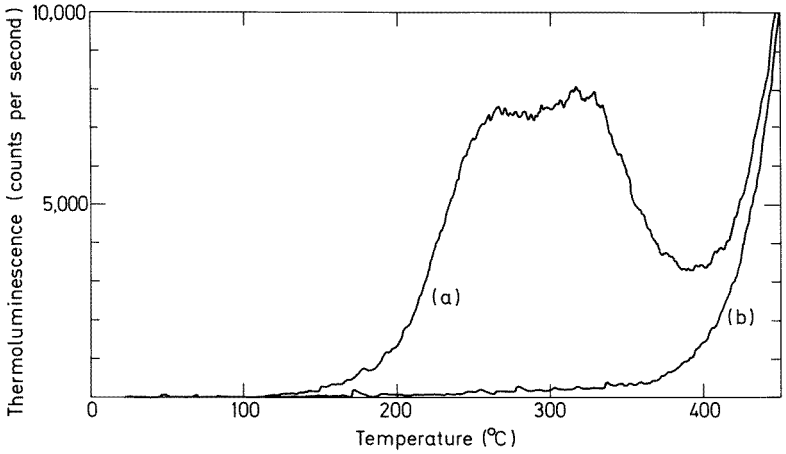

Figure 10. TL glow-curve observed from a small sample taken from an Etruscan terracotta statue (measurement by D Stoneham (1984 personal communication). Curve (*a*) shows the light emission observed during the first heating, and curve (*b*) the light observed during a second heating. The latter is the red-hot glow, or incandescence, that occurs whenever a sample is heated, but during the first heating there is substantial TL in addition. The glow-curve was obtained by placing a grain-carrying disc on an electrically heated nichrome plate servo-controlled to give a rate of temperature rise of 20 °C s^{-1} (from Aitken 1985).

3.1.2. Measurement of luminescence. The basic requirements for measurement of the signals are a wide solid angle of light collection and a detector having low electronic noise. Up to the present these have been met by a photomultiplier with a bialkali photocathode of diameter 5 cm placed close to the sample (so as to obtain a solid angle of collection approaching π sr); the commonly employed device is the Thorn-EMI 9235Q (successor to the 9635Q) for which dark count-rates of the order of 10 s^{-1} can be achieved by careful selection. The signal is taken from the anode of the photomultiplier in photon-counting mode rather than DC mode; the essential basis of data handling is a multichannel analyser in which the counts from the photomultiplier are stored in sequential intervals of time (for OSL) or temperature (for TL). It is possible that charge-coupled devices (CCDs) will eventually supersede photomultipliers but at present these are used mainly for special purposes such as spectral measurements and single-grain luminescence.

Between collection and presentation for measurement the sample is subjected to comprehensive pretreatment inclusive of separation into mineral and size fractions; this must be done in very subdued long-wavelength light in order to avoid 'bleaching' of the signal. The end product is upwards of a dozen portions (aliquots) of grains on aluminium or stainless steel discs (typically 10 mm diameter, 0.5 mm thick); for various reasons these need to be monolayers, particularly for OSL, and depending on grain size the number on a disc may be in the region of a few hundred to a few thousand.

Thermoluminescence. Figure 10 shows an example of a TL glow-curve. A crucial feature of TL measurement is suppression of so-called 'spurious' TL. This is not induced by radiation and is a surface phenomenon which is not well understood—prior inter-grain friction plays a part but there are other influences as well. Fortunately it can be avoided if the TL oven is flushed with high purity nitrogen or argon, after removal of air; elimination is also enhanced by red-rejection colour filters.

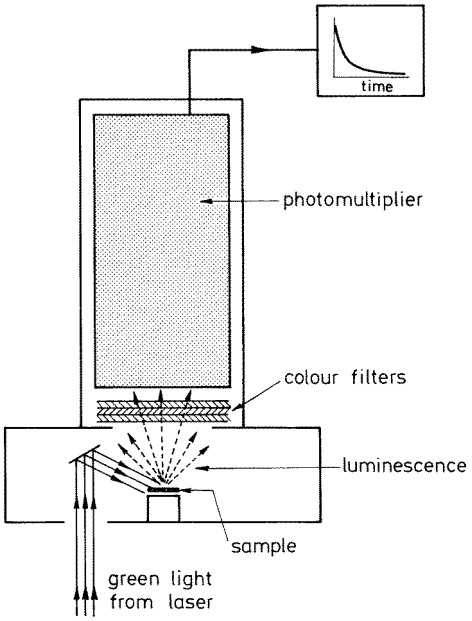

Figure 11. The basic experimental arrangement for measurement of OSL (as first used by Huntley *et al* 1985). In order to prevent scattered laser light from swamping the weak wanted signal from the sample it is necessary to insert, in front of the photomultiplier, colour filters that give severe rejection of green light but which pass blue, violet, and near-UV wavelengths. Nowadays measurement facilities are automated (see figure 12).The signal from the photomultiplier anode decays rapidly from the moment of laser switch-on because of depletion the trapped electrons; with typical intensity of the laser beam the signal decreases by a factor of two in about 10 s (from Aitken 1990).

The glow-curve from a sample in which there is only one trap type consists of a broad peak but in practice several trap types are usually present in a sample and the glow-curve consists of a number of overlapping peaks. In general terms the greater the trap depth, E, the higher the temperature at which the resultant peak occurs; also, the electron-retention lifetime is longer. For archaeological or geological dating the glow-curve region of interest is upwards of 300 °C; below this temperature the TL is from traps that so shallow that they will have suffered serious loss of electrons during the centuries of burial. Unfortunately for some minerals, notably feldspars and zircon, there is the possibility of leakage during burial even from deep traps (Wintle 1973), particularly with samples of volcanic origin; as might be expected this manifests itself also with OSL. One explanation of this malign phenomenon—*anomalous fading*—is that there is leakage by wave-mechanical tunnelling. Experimentally there are indications that such leakage does not occur with traps associated with luminescence centres that emit in the far red (Visocekas and Zink 1999).

Optically stimulated luminescence. In using light for stimulation of luminescence it is crucial that the intensity of the background of photons scattered by the sample is small compared with the weak wanted signal of luminescence. In the initial development of the technique (Huntley *et al* 1985) green light from an argon ion laser was used for stimulation; the basic experimental arrangement is indicated in figure 11. The colour filters in front of the photomultiplier give severe rejection of green light, by a factor of the order of 10^{24}, but pass violet and near-UV wavelengths carrying the wanted signal; only anti-Stokes luminescence, i.e. light of shorter wavelength than the stimulating photons, is useful for dating. The foregoing refers to the prompt luminescence emitted during stimulation as has been used for nearly all dating measurements; an alternative is to use delayed luminescence (phosphorescence) and studies of this on a nanosecond timescale are proving useful in elucidation of mechanism (e.g. Clark and Bailiff 1998).

Light from a laser remains the preferred source for stimulation of quartz but other less

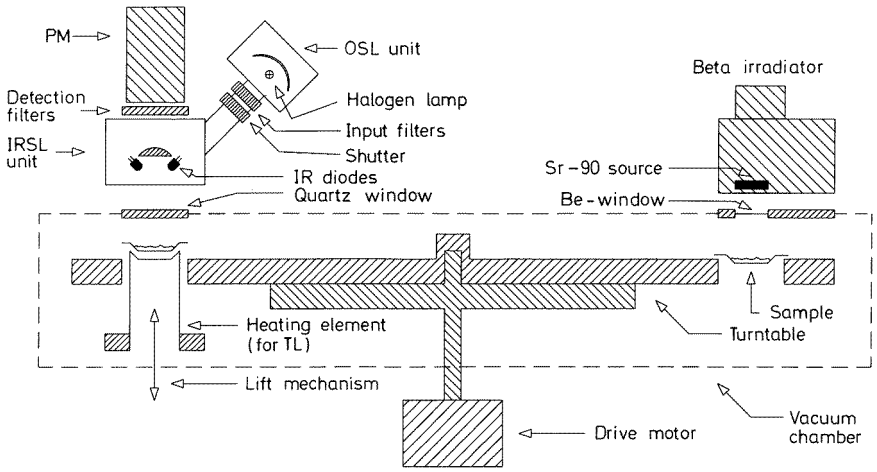

Figure 12. Combined OSL and TL measurement facility (developed by the Risø National Laboratory, Denmark; diagram kindly provided by L Bøtter-Jensen). The basic device consists of a turntable in which there can be up to 48 positions for loading aliquot-carrying discs; the table rotates in steps and when a disc reaches the position of the lift mechanism it is raised for measurement of luminescence. Stimulation of OSL can be either by filtered light from the halogen lamp or by infrared from the array of 23 IR diodes; alternatively green or blue diodes can be mounted. The beta irradiator is positioned diametrically opposite to the measurement position; an alpha irradiator can also be incorporated. Preheating can be carried out on the heater strip. The system is fully automated allowing the sequence of irradiation, preheating, and measurement to be completed with minimal attention. Prior to a TL run the chamber is evacuated and filled with high-purity nitrogen so as to avoid spurious luminescence. The overall diameter of the chamber is 30 cm (from Aitken 1998).

expensive sources are now in common use: xenon and quartz-halogen lamps appropriately restricted in wavelength range by colour and interference filters; green- and blue-emitting diodes. For feldspars there is a stimulation resonance centred on 860 nm and this allows the use of infrared-emitting diodes. At first sight it is surprising that photons of quantum energy 1.44 eV (corresponding to a wavelength of 860 nm) are able to evict electrons from traps deep enough, say with $E = 1.6$ eV, to have long enough retention lifetimes; thermal assistance, in the form of lattice vibrations, supplies the deficit (Hütt *et al* 1988, Bailiff 1993, Godfrey-Smith and Cada 1996).

The TL glow-curve (see figure 10) gives separation of luminescence associated with deep traps from that from shallow ones and it is of course the former that have lifetimes that are long compared with the burial age of the sample. With OSL there is no equivalent of the glow-curve and it does not prove possible to avoid shallow-trap luminescence by choice of stimulating wavelength. Instead it is necessary, by *preheating*, to guard against contamination of the artificial signal by luminescence from traps that do not contribute to the natural signal.

For reliable dating it is necessary to make many measurements and consequently automation is highly advantageous; figure 12 shows one of the commercially available systems incorporating both OSL and TL facilities.

3.1.3. Radioactivity; artificial irradiation. Potassium, thorium, and uranium are usually the principal contributors to the dose-rate; there are also contributions from rubidium and cosmic rays. Dose-rates are derived from nuclear data tables on the basis that, within a volume having dimensions greater than the ranges of the radiations, the overall rate of energy absorption is

equal to the rate of energy emission (for a recent update of values see Adamiec and Aitken 1998).

The isotope of potassium that is radioactive is ^{40}K with a natural atomic abundance of close to 0.01%. It emits both beta particles and gamma rays; from uranium and thorium there are alpha particles in addition. Because these are heavily ionizing they are less efficient, on an absorbed energy basis, in inducing latent luminescence than the two lightly ionizing radiations and hence the response of a sample to alpha particles has be assessed separately from the response to lightly ionizing radiations. Commonly, ^{241}Am is the radioisotope used for assessment of the alpha particle response and beta particles from ^{90}Y for that of the lightly ionizing particles.

Another complication with alpha particles is on account of their short range—the order of 20 μm in pottery or sediment; thus in a 100 μm grain that is free of uranium and thorium it is only the outer rim that is irradiated. This dictates selection of two categories of grain size for measurement: either fine grains of less than 10 μm, or coarse-grains of upwards of 100 μm. The former receive the full alpha dose rate; for the latter the alpha-irradiated rim is etched off with hydrofluoric acid; in a not untypical sediment the respective dose-rates are around 2 and 1.5 Gy ka^{-1}. This latter assumes that the grains themselves are free of radioactivity—a good approximation for quartz but for potassium feldspar there is a significant internal beta dose-rate for coarse grains.

Assessment of dose-rate. The dose-rate from thorium and uranium is provided not only by ^{232}Th, ^{235}U and ^{238}U, but also by the chains of radioelements that follow those parents. The half-lives of the parents, as well as of ^{40}K and ^{87}Rb, are all in excess of, or close to, 10^8 years and hence there is no change in burial dose-rate resulting from radioactive decay—as long as the chains remain in radioactive equilibrium; this latter condition can be upset by leaching due to groundwater percolation or by escape of the gas radon which occurs halfway down the ^{238}U chain.

A range of techniques is available for elemental determinations; these include neutron activation, atomic absorption, x-ray fluorescence, flame photometry, and inductively coupled plasma mass spectrometry (ICPMS). The disadvantage of this as the sole approach in respect of thorium and uranium is that the evaluated dose-rate may be significantly erroneous if the decay chains are not in equilibrium. So it is necessary to check this, usually by high-resolution gamma spectrometry, or by alpha spectrometry. Both of these measure the activities of several individual radionuclides in the decay chains and hence determine the degree of disequilibrium, if any. Distortion by disequilibrium is reduced if direct measurement of radioactivity is made, such as by particle counting or thermoluminescence dosimetry (TLD). The latter is used for on-site measurement of gamma dose-rate, an alternative being a portable a portable gamma spectrometer.

3.1.4. The advantage of OSL over TL for unburnt sediment. Although TL has the convenience of the glow-curve in respect of stability indication, for types of sample for which the dated event is the last exposure to daylight, such as unburnt sediment, there is strong advantage in using OSL. This is because the TL signal comprises luminescence from traps irrespective of their bleachability—their susceptibility to emptying by photons. For OSL the nature of the stimulation ensures that only easily bleachable traps are sampled. This means that to a first order there is no residual of latent OSL immediately after deposition of sediment whereas for the latent TL the residual is liable to be substantial—because of the sampling of unbleachable traps. Also, the amount of exposure to photons needed to reach the near-zero level of latent

OSL is very much less than that needed to reach even the substantial residual level of latent TL; this is particularly important for sediment that is deposited from suspension in water—not only is the overall light intensity less but also the spectrum is deficient in short wavelengths which are more effective at bleaching.

There are also methodological advantages in the use of OSL. These stem from the feasibility of sampling the traps by means of a short stimulation, with only minor depletion of the content. This allows measurement of paleodose on a single portion of sample, even on single grains (e.g. Lamothe *et al* 1994, Murray and Roberts 1997, Duller *et al* 1999). Such measurements allow grain-by-grain paleodoses to be obtained for a sample and hence incisive indications about the circumstances of a sediment's deposition are obtained, as illustrated by the example below.

The Jinmium rock shelter, northern Australia. The time of first human arrival on the Australian continent is of considerable interest in Aboriginal studies as well as for human development on a global scale. Radiocarbon dating had placed this arrival at around 40 000 years ago—roughly that technique's limit. When TL and OSL had been applied to the lowest artefact-bearing sediments on two sites dates in the range 50 000–60 000 years ago were obtained; these were acceptable to some archaeologists though strongly resisted by others. Subsequently, quite iconoclastic claims for a much earlier human presence were made on the basis of TL ages in the range 116 000–176 000 years ago for artefact-bearing sediments at the Jinmium rock shelter (Fullagar *et al* 1996).

Following critical comment on these old ages (Bahn 1996, Roberts 1997, Spooner 1998) OSL was used to date single grains of quartz. A substantial spread in paleodose was found and this was interpreted as being primarily due to the admixture, at deposition, of grains that had not been well bleached (Roberts *et al* 1998, 1999). Three categories of grains were hypothesized: some that had been well bleached, some (predominating) that had been partially bleached due to insufficient exposure to daylight, and, a few that had not been bleached at all—because they had been released into the deposit by weathering from the rock walls and from rock rubble. After statistically based exclusion of these high-age grains (Galbraith *et al* 1999) it was concluded that the entire deposit was formed less than 10 000 years ago. The OSL ages were in agreement with radiocarbon for the upper part of the deposit but there was no charcoal in the more crucial lower part relevant to first human occupation.

3.2. Electron spin resonance (ESR)

3.2.1. Outline. With TL and OSL, eviction of electrons from traps is an integral part of the measurement process; with ESR eviction does not occur and the presence of trapped electrons is detected by their response to microwaves in the presence of a strong, steady magnetic field which is slowly changing. For a given frequency there is a certain value of magnetic field at which transitions are induced between different spin states of unpaired electrons; detection of this resonance is indicated by absorption of microwave power and the greater the number of electrons the greater the absorption. Hence the power absorbed is a measure of age and as with TL and OSL the paleodose can be determined by comparison of this signal with that induced by laboratory irradiation.

Transitions occur when the energy difference between two spin states in the applied magnetic field equals the quantum energy of the microwaves. The magnetic field, B, at which this occurs in microwaves of frequency ν is given by

$$g\beta B = h\nu \tag{3b}$$

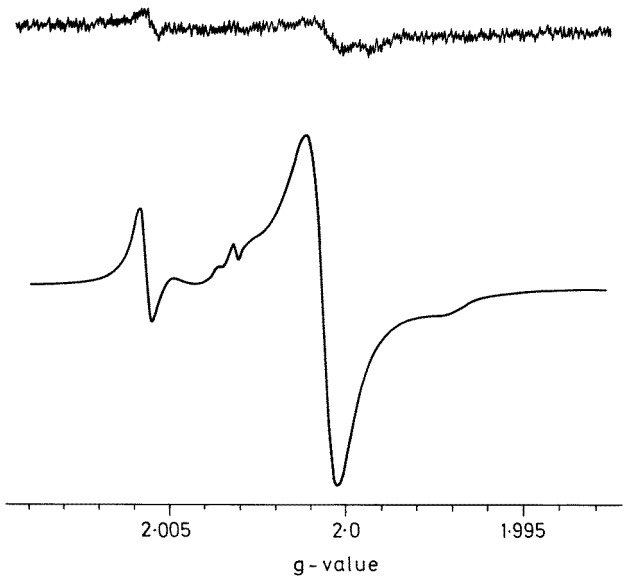

Figure 13. ESR signals from young calcite (above) and older calcite (below); the upper signal has been amplified by a factor of 10. A plot of the absorption would be a single peak but for precision of measurement it is advantageous to use the first derivative of that plot; the strength of the signal is measured as the vertical distance between the positive peak and its associated negative peak (modified from Grün 1997).

where h is Planck's constant, and, $(g\beta B)$ is the energy difference between the two levels, β being the value of the Bohr magneton, and $g = 2.0023$ for free electrons.

In a solid the g-value is different to that for free electrons because of interaction between the electron spin and the lattice but for the paramagnetic centres relevant to ESR the g-value is still close to 2. Unlike the situation in luminescence, the nature of the defects concerned in ESR, i.e. the paramagnetic centres, is usually known. Alternatively the process is described as electron paramagnetic resonance (EPR).

The technique is of particular importance in application to tooth enamel on Palaeolithic sites, as further discussed below. It has also been used for materials such as stalagmitic calcite, mollusc shells, and coral; time zero corresponds to formation of the crystals concerned. In general, the age range is upwards of a million years—substantially greater than for the luminescence techniques. On the other hand it is less sensitive in response to radiation dose so that the minimum age that can be measured is less recent.

Reviews of the archaeological and other usages of ESR include those by Grün (1997) and Ikeya (1994). In retrospective dosimetry of nuclear events, such as at Hiroshima and Chernobyl, ESR measurements on tooth enamel and buttons made of shell have been used to give direct assessment of the dosage received by humans.

3.2.2. Measurement. The sample is positioned in a microwave cavity between the poles of an electromagnet; for a frequency of 9 GHz (X-band) equation (3*b*) indicates that a field of 0.32 T is required for resonance; for 35 GHz (Q-band) the required field is 1.25 T. A sample size of a fraction of a gram is typically used. The form in which the signal is obtained is indicated in figure 13.

Some form of preheating, such as a few days at around 100 °C, is employed before

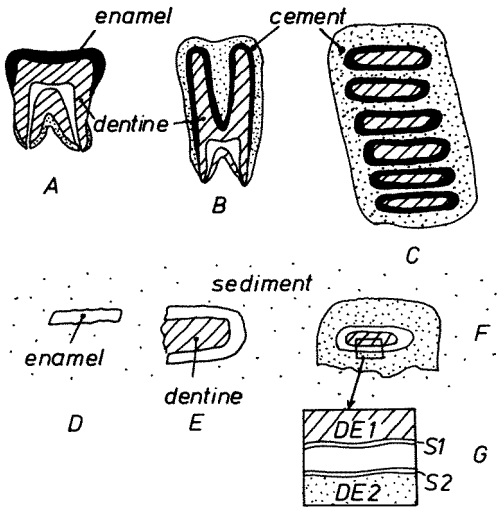

Figure 14. Types of mammal teeth (A: human, B: camel, C: elephant) and some possible burial situations. In G, the sources of dose-rate external to the enamel (central layer) are marked DE1 (dentine) and DE2 (sediment); S1 and S2 indicate removal of the enamel surface so as to avoid the alpha-particle contribution from dentine and sediment (modified from Grün 1997).

measurement in order to empty shallow traps that, after laboratory irradiation, would otherwise give rise to a contaminant signal. Since each type of defect has a characteristic g-value, in principle this is not necessary; however it is often the case that the unwanted signal has such close proximity in g-value to the wanted signal that there is interference.

A rough estimate of the stability of a given wanted signal can be made by measuring the electron-retention lifetime for a series of elevated temperatures (in the range 150–200 °C) so as to reduce the lifetime to a span of days rather than millions of years. Then on the basis of the Arrhenius equation

$$\tau = s^{-1} \exp(E/kT) \tag{3c}$$

the lifetime at the presumed burial temperature is found by extrapolation; however because the degree of extrapolation is severe this gives only a rough estimate. In equation (3c) τ is the lifetime at T K, s is a frequency factor related to the lattice vibrational frequency, and k is Boltzmann's constant. An alternative is to measure the equilibrium paleodose in very old samples of the same type.

3.2.3. Dose-rate. The essentials of dose-rate determination are the same as for the luminescence techniques but in practical application the nature of the prime type of sample for ESR dating, tooth enamel, introduces severe microdosimetrical complications. In dating skeletal remains enamel is chosen rather than bone or dentine because in the latter two there is continued mineralization many millennia after death with the consequence that time zero for much of the ESR signal is subsequent to death.

The geometry of some mammal tooth is illustrated in figure 14 and from this it will be seen that besides the radioactivities of the enamel itself and of the sediment in which the tooth has been buried there will be a contribution to the dose-rate from the radioactivity of the dentine; in fact this turns out to be of dominant importance because of the high uranium content of dentine in long-buried teeth. Potentially there are components due to both alpha and beta particles but the complication of the former is eliminated by grinding off the outer 50 μm layer of the enamel; the dentine beta component is complex enough!

This complexity arise in two ways. First, the uranium content in the dentine of a long-buried tooth may be several hundred times that in that of a tooth of a just-dead mammal

and hence the corresponding final dose-rate will be different to the initial dose-rate; a similar situation occurs with the uranium-series dating of bone (section 2.3.3). In the early uptake (EU) model it is assumed that the uranium entering from the burial soil reached full value soon after burial; in the linear uptake (LU) model it is assumed that the final value was reached by linear increase with time starting at zero at the time of burial. Ages are calculated on the basis of these alternative scenarios; if the dose-rate from the internal uranium is large compared the gamma dose-rate from the surrounding soil the EU age is substantially less than the LU age.

The second type of complexity is more amenable to remedy. As we have seen in section 2.3 after uptake of uranium there is gradual 'grow-in' of ^{230}Th and subsequent members of the uranium chain (see figure 7). In the case of EU most of this occurs during the first 100 000 years and during this period the internal dose-rate approximately doubles, but this increase is amenable to calculation.

Combined ESR and uranium-series dating. As described in section 2.3, uranium-series dating presumes early uptake of uranium; if in fact the LU model is closer to reality the derived age, on the basis of EU, will be too small. Ages can be evaluated on the basis of various uptake scenarios and the same can be done for ESR; agreement is indicative of the correct scenario. Application of this approach to several sites in Israel spanning 50 000–150 000 years ago indicated that the mode of uptake varied from site to site (McDermott *et al* 1993); the study also confirmed the conclusion based on TL dating of burnt flint that early modern *Homo sapiens* lived contemporaneously with Neanderthals rather than the former being descendants of the latter.

3.3. Fission tracks

3.3.1. Outline. When ^{238}U, the parent of the major series in natural uranium, undergoes spontaneous radioactive decay there is a small probability that instead of emitting an alpha particle its nucleus will undergo fission into two roughly equal fragments. These fragments recoil from each other and for uranium atoms located in a number of minerals (and glasses) the fragments cause substantial disruption in the structure of the host lattice, leaving tracks that are around 10 μm long. These can be made visible under the microscope by prior etching with an appropriate chemical reagent (e.g. molten KOH–NaOH in the case of zircon) because the damaged regions are more vulnerable to attack; the etching also reveals other imperfections in the structure but these are distinguishable.

Heating anneals the tracks and it is such an event in antiquity that sets the clock to zero—hence, like the K–Ar method it is primarily applicable to volcanic products and archaeological dating is nearly always indirect (though there have been a few applications to samples heated by fire). For zircon an hour at around 800 °C is necessary for zeroing but for most other minerals and glasses a lower temperature is sufficient. Thereafter the number of tracks grows with time and the number accumulated in a sample is a measure of its age. Obviously it is also necessary to know the amount of uranium present, the rate of spontaneous fission, and some measure of the probability that an observable track will result from a fission event.

Though there are some minerals for which fading or saturation gives an upper limit to the attainable age it is the lower limit that is restrictive as far as archaeology is concerned, simply due to sparsity of tracks. This limit is determined by the uranium content and the diligence of the operator; typically with uranium content in the range 1–10 ppm, as for obsidian, around 20 000 years can be reached but this can be extended by the procedure of repeated grinding and etching, thereby exposing fresh areas for counting. An obsidian knife blade, for which there was evidence of heating in antiquity because of its distorted shape, has been dated by Fleischer

et al (1965) using 36 fresh surfaces, giving an age of 3700 (±900) years—random fluctuations in the decay process set a limit to the precision attainable quite apart from other uncertainties. For zircon the uranium content is in the range 100–1000 ppm and the corresponding lower limits are in the range 1000–100 years.

An incidental use of fission-track dating dating is in the identification of tephra layers far from the volcanic source; an example of this (Westgate *et al* 1998) is in respect of a widespread layer occurring across peninsular India but emanating from a volcanic eruption in Sumatra about 75 000 years ago.

3.3.2. Measurement. After etching, the tracks can be observed, and counted, with an optical microscope having magnification in the range ×500–2500. The amount of uranium present in the given microsample and the probability of recording an event are assessed by means of counting the fission tracks induced by exposure to thermal neutrons in a nuclear reactor; such induced fission is from ^{235}U, present in natural uranium with an atomic abundance of 0.72%. As long as the track density is far from saturation the age is given by

$$T = (\rho_s/\rho_i)(\phi I \sigma/\lambda) \qquad (3d)$$

where ρ_s is the track density from spontaneous fission during burial, ρ_i is that from induced fission due to a thermal neutron fluence ϕ, σ is the fission cross section, I is the isotopic ratio of ^{235}U to ^{238}U, and λ is the rate of spontaneous fission. An alternative to direct measurement of the latter, which is difficult, is to make simultaneous measurement of a known age standard—which also obviates the need for measurement of the neutron fluence as well as I and λ.

The above (*population method*) requires that the uranium distribution in the sample is uniform, such as in volcanic glass, because two portions are needed—one for measurement of ρ_s and the other for measurement, after irradiation, of the additional tracks, ρ_i. For minerals such as zircon in which the uranium distribution is heterogeneous the external detector method (EDFT) is used. After measurement of ρ_s the sample is mounted against a cleaved sheet of low-uranium mica and irradiated; the value of ρ_i is obtained from the tracks in the mica made by fission fragments that have traversed the sample–mica interface. Single grains of zircon can be dated in this way, as long as they are not too small (>75 μm); each grain in the subsample is matched against its corresponding induced-track print on the external detector. As with the K–Ar method such single-grain dating allows separation of the components of a mixture of grains of different ages.

Alpha-recoil tracks. A severe limitation in application of fission-track dating to more recent archaeology than concerned with hominid evolution is that there are usually too few tracks—because of the low rate at which fission occurs. Emission of alpha particles is many orders of magnitude more frequent and these too leave recognizable tracks in some minerals. The tracks are very much shorter and consequently rather difficult to distinguish from imperfections; nevertheless there is the possibility that this could be developed into an important technique with some minerals.

3.3.3. Fading. Although in zircon and sphene the tracks have good stability, in most other types of sample there is a spectrum of stabilities and as might be expected it is only those that do not fade during laboratory heating until a temperature of a few hundred degrees is reached that are sufficiently robust to survive for long burial times; obviously in equation (3*d*) it is required that the ratio (ρ_s/ρ_i) refers only to robust traps. There are various stratagems for ensuring this.

In the *plateau method* the two portions (in the population method) are subjected to successive annealings of increasing stringency and the ratio (ρ_s/ρ_i) plotted against temperature (if a fixed duration of heating is used), or duration (if the temperature is fixed). The ratio gradually rises and if a constant value — a plateau — is reached then this is indicative that at the onset of the plateau the annealing has been sufficient to remove the same percentage of tracks from the irradiated portion as faded from the natural portion during burial; hence the plateau value of (ρ_s/ρ_i) gives the correct age.

Another approach is by measurement of track size. When fading has occurred the tracks remaining are smaller than fresh tracks and it is possible to relate the percentage that have disappeared to the diminution in size. In the isothermal plateau fission-track (ITPFT) method, applicable for samples having uniform uranium content, there is a single heat treatment, such as 150 °C for 30 days, and coincidence in the size distributions of the spontaneous and induced tracks is used as indication that the plateau value of (ρ_s/ρ_i) has been reached.

Further details of the ITPFT and other methods will be found in the review by Westgate *et al* (1997).

4. Chemical change

All around us we have evidence of chemical and biological degradation as time passes; yet, because such changes are highly dependent on temperature and to a lesser degree on other environmental factors, the development of consequent systems of dating are not easy to achieve.

4.1. Amino acid racemization (AAR)

4.1.1. Outline. The constituent amino acids of proteins can exist in two forms which are chemically equivalent but structurally different: the D form which rotates the plane of polarized light clockwise, and the L form for which the rotation is counter-clockwise. On formation in living organisms—primarily bone, teeth, and shell in the context of dating—the acids are in the L form and, on account of continual replacement, remain so until death. There is then slow conversion to the D form until, because of reverse conversion, an equilibrium ratio is reached; the mixture is then said to be *racemic* and in the simplest case the ratio is unity. The extent to which the D/L ratio has risen from zero towards the equilibrium value is the basis of dating. The ratio used to be evaluated through the difference in optical activity of the two forms but chromatography is now preferred, of which the method of choice is high-performance liquid chromatography (HPLC).

Of the various possible acids the most used have been aspartic, alanine, and isoleucine. For aspartic the D/L ratio reaches 0.5 in around 400 000 years at 0 °C and 3000 years at 25 °C; for alanine the corresponding values are the order of a 1 000 000 years and 10 000 years. For isoleucine the conversion is slower still with corresponding values of the order of 6 000 000 years and 50 000 years; in this case the conversion process is more strictly called *epimerization* and the conversion is from L-isoleucine to D-alloleucine. Besides L to D conversion there are several other types of protein diagenesis that are useful, such as the hydrolysis of leucine.

Calibration. It is possible by laboratory measurement following storage at elevated temperatures to determine the rate constant for the process as a function of temperature; coupled with estimates of site temperature throughout the burial period, evaluation can then be made of the years that have elapsed since the process began. However, it has been found more reliable to use the alternative calibration approach in which the rate constant is found by

measurements on samples for which the age is known by other means, usually radiocarbon; the calibration samples need to be of the same type as those used for dating and from the same site so that environmental factors, notably temperature, are the same.

One may distinguish two cases: interpolation and extrapolation. The former is relevant to situations in which not many radiocarbon dates are available either because suitable samples are sparse or because of cost—a radiocarbon determination is substantially more expensive than an AAR measurement. Given the greater age range of AAR, extrapolation is the more common need and then careful consideration needs to be given to the question of whether the factors are likely to have been the same in the extrapolated time period; when this bridges a glacial–interglacial boundary it may be necessary to be content with maximum and minimum ages according to the assumptions made about past climate. In principle, the temperature problem can be circumvented by using two acids having different rate constants, and differing temperature dependences: only one combination of age and temperature fits the two observed D/L ratios.

Distorting influences. Besides dependence on temperature the conversion rate can also be affected, particularly when using aspartic acid from bone, by water and its acidity as well as on the degree of protein degradation; the latter also favours the ingress of contaminating amino acids from ground water. On the other hand there are materials such as tooth enamel and ostrich eggshell that are more much more impervious; also, use of isoleucine is advantageous on account of it being hydrophobic. With the availability of increased specificity in measurement a greater range of acids is becoming available, allowing in-depth studies of the complex degradation processes (for a review, see Hare *et al* 1997).

Burning and boiling. In dating animal bones there is the risk that they may have been cooked, thereby increasing the D/L ratio and giving an erroneously high age; similarly with cremation and with eggshells that have fallen into the fire. Sometimes there is visual evidence of such heating; sometimes it can be detected by looking for the absence of particular heat-sensitive components of protein; finally it can be checked by the use of two reactions having different rate constants and temperature dependences (Miller *et al* 1992).

Measurement of D/L ratios can also be used for determining thermal histories. A novel example is the use of the aspartic acid ratio to establish that the corpse of the German Emperor Lothar I was boiled before burial. This emperor died, in AD 1137, some 500 km from his castle; it was hypothesized that because of the delay in returning his corpse to the castle for burial it was defleshed by boiling in order to avoid putrefaction. Comparative D/L ratio evaluations on the emperor's bones and those of relatives known to have died close to the castle indeed showed a clearly enhanced ratio for the former, consistent with about 6 h boiling (Bada *et al* 1989).

4.1.2. Dating the extinction of Australian megafauna (Miller et al 1999). The eggshells of large, flightless birds (ratites) are a particularly good material for the application of AAR and this has led to an important insight into the circumstances of their extinction in Australia—a facet of the comparatively recent disappearance in many regions of the world of '. . . the hugest, and fiercest, and strangest forms . . . ' of animal life—to quote the explorer Alfred Russell Wallace. The outstanding question for many decades has been whether the demise was the result of climate change or alternatively through human intervention. Unlike bone such eggshells are well preserved and their dense calcite matrix is resistant to diffusional change. Hence in addition to AAR they are good material for radiocarbon and uranium-

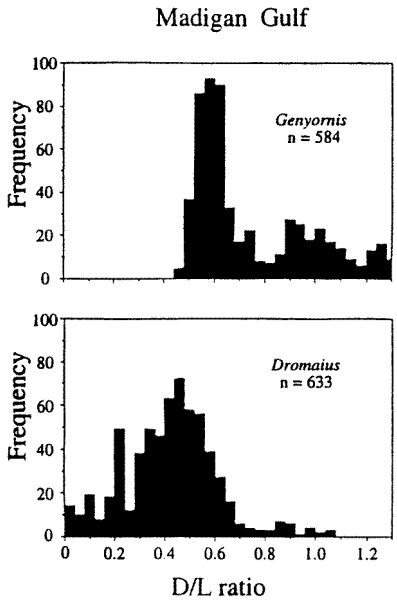

Figure 15. Histograms of the D/L ratio for ancient eggshells of the mihirung (*Genyornis*) and of the emu (*Dromaius*) from the Madigan Gulf region of Australia. Calibration against uranium-series and luminescence dating indicates that the minimum D/L ratio for the mihirung, i.e. its extinction, corresponds to 50 000 years ago (modified from Miller *et al* 1999).

series measurements using the AMS and TIMS techniques, respectively (section 2.1.2 and section 2.3.2); all three allow application to a single fragment of shell. Together with optical dating (section 3.1) of associated sediment these absolute techniques provide a firm basis for AAR calibration with avoidance of the need for extrapolation and its inherent uncertainties.

The epimerization of isoleucine was used for AAR and the species studied were the now-extinct ostrich-sized mihirung (*Genyornis newtoni*) and the surviving emu (*Dromaius novaehollandiae*); eggshells were obtained from three regions of differing climate. In all there was a continuous distribution of D/L ratios for the emu, from zero to around unity, whereas for the mihirung the ratios were all upwards of 0.3–0.5; the values for one locality are shown in figure 15. After calibration it was concluded that extinction of the latter occurred about 50 000 years ago, the spread in minimum ratios being due to the different climatic regimes.

As noted in section 3.1, the time of arrival of humans in Australia is now widely accepted as around 50 000–60 000 years ago and this suggests that the demise was the result of human intervention. Miller *et al* (1999) propose disruption of the ecosystem as the dominant mechanism, perhaps coupled with human predation. The differing dietary preferences of the mihirung and the emu are adduced as explaining the extinction of the former and the survival of the latter; measurement of the ratio between the stable isotopes ^{13}C and ^{14}C in the eggshells indicated that the mihirung was primarily a browser of shrubs and trees whereas the emu had wider dietary tolerance—its acceptance of grasses enabling it to survive despite severely decreased availability of shrubs and trees. The authors postulate that human burning at times of the year and at frequencies to which the vegetation was not pre-adapted was the cause of this decrease in availability.

4.2. Some other chemical methods

Obsidian hydration. Obsidian is a form of volcanic glass widely used for prehistoric tools and weapons. The basis of dating is that a freshly chipped surface slowly acquires a hydration rim by diffusion into it of water; depending on age, burial temperature and composition, the thickness of the hydrated layer found on excavated obsidian is likely to lie in the range 1–50 μm

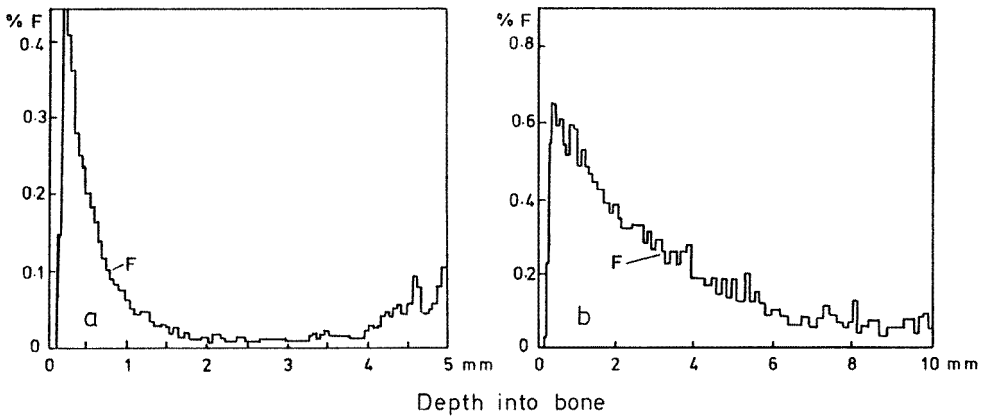

Figure 16. Nuclear microprobe profiles of fluorine: (*a*) from a 700 year old bone, and (*b*) from a 16 000 year old bone. Dating is based on comparison with theoretical diffusion profiles calculated for different ages (from Aitken 1990).

and to be measurable by optical microscopy. For some regions, e.g. New Zealand, the growth is rather slow and for objects that were chipped only a few hundred years ago the layer may be below this range; this has lead to trial of utilization of nuclear resonance reactions (Leach and Naylor 1981) and of sputter-induced optical spectrometry (Leach and Hamel 1984).

Bone. The progressive degradation of buried bone causes difficulties in application to that material of other techniques but the same degradation can be used to give rough age indication. With the disappearance of protein the nitrogen content decreases and conversely there is increase in the fluorine contents due to incorporation into the phosphatic mineral (hydroxyapatite) of which bone is mainly composed. Also, as has been noted in section 2.3.3, uranium is insignificant in living bone but the content becomes substantial during burial; an early technique (Oakley 1955) was based on beta activity; this increases with burial time both on account of uranium uptake and the grow-in of beta-emitting daughters (see figure 7).

Unfortunately, the changes in bulk content are strongly dependent on burial environment but at any rate in the case of fluorine the diffusion profile is nevertheless usefully diagnostic of age—as illustrated in figure 16. The profiles were obtained using a nuclear microprobe employing 2.5 MeV protons to produce 6–7 MeV gamma rays from the fluorine (Coote *et al* 1982).

5. Changes in the Earth's magnetic field

5.1. Outline

The magnetic compass has long been used for navigation and we learn from written records that for several centuries there has been the realization that magnetic North differed from geographic North by a varying amount. From the nineteenth century onwards past variations have been studied through the recording mechanism of thermoremanent magnetism (TRM) acquired by iron oxide in baked clay and volcanic rocks on cooling from around 700 °C. Such magnetization has remarkable stability and is the basis of archaeomagnetic dating using oriented samples taken from the baked clay walls of pottery kilns. This is useful in archaeological dating over the last two or three millennia; it utilizes the secular variation of direction—swings of the order of 10°

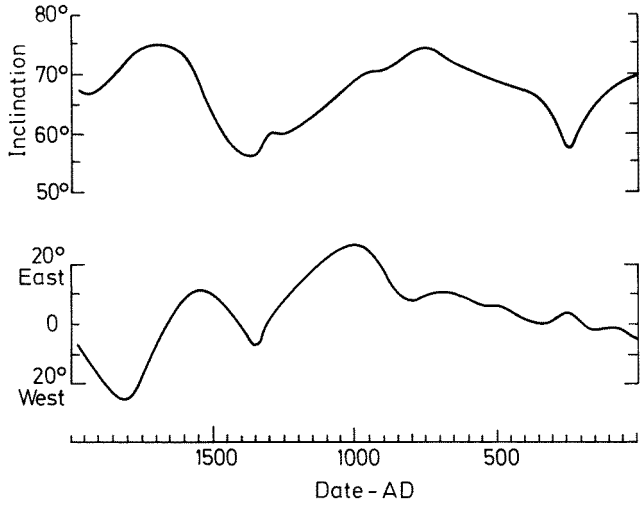

Figure 17. Direction of the Earth's magnetic field in southern Britain according to archaeomagnetic measurements (Clark *et al* 1988), and from AD 1576, according to observations recorded by scientists. The lower section shows the declination (D)—the angle between Magnetic North and True (Geographic) North. The upper section shows the inclination (I), or angle of dip—the angle by which the north-seeking end of a magnetized needle suspended at its centre of gravity points below the horizontal (from Aitken 1990).

or so in declination and inclination as illustrated in figure 17. On a much larger scale, both in time and in extent, are reversals of direction of the magnetic field and these are the basis of the worldwide polarity timescale which now extends back over millions of years; in addition to the TRM of volcanic rocks the detrital magnetization of unburnt sediment is important here, as indeed to some extent in archaeomagnetic dating.

Sediments. A weak but stable magnetization is acquired by sediments when deposited from calm water due to the tendency of already magnetized particles to align in the geomagnetic field as they settle. Post-depositional remanent magnetism (PDRM) is of more widespread interest. One form this arises from is alignment of particles while the sediment is still in the form of a slurry, becoming locked as the sediment consolidates. Another form is chemical remanence (CRM) acquired through the formation of a new magnetic mineral (e.g. the reduction of haematite to magnetite); there is alignment of domains as the new mineral forms—as also occurs in the magnetite synthesized by certain types of bacteria.

Measurement. Delicately suspended magnets were initially used as detectors and subsequently spinner magnetometers were introduced; in these the signal is the minute voltage induced by rotating the sample inside the coil system; alternatively fluxgate elements are used for detection. Ultra-high sensitivity is now provided by the SQUID cryogenic magnetometer; this superconducting quantum interference device utilizes the Josephson effect and operates at the temperature of liquid helium.

Ancient intensity. There is proportionality between the intensity of the TRM and the strength of the field in which it is acquired. Hence the latter can be determined by comparing a

sample's as-found magnetization with the TRM it acquires after heating and cooling in a known laboratory field; alternatively microwaves can be used for remagnetization (Walton *et al* 1993).

In the past there has been substantial variation in field intensity—between 1000 and 500 BC it reached a value some 50% higher than at present. While this is useful as an adjunct to directional dating, a more important aspect of past variation is in understanding, and estimating, the distortion of the radiocarbon timescale; the field intensity influences the cosmic-ray flux in the upper atmosphere, and hence the production rate of radiocarbon. For this purpose values from sediment are used as well as from volcanic rocks. These are relative rather than absolute values since it is not possible to make laboratory simulation of the deposition process by which the sediment magnetization was acquired.

5.2. Secular variation; archaeomagnetic dating

Figure 17 shows the irregular way in which the direction of the magnetic field, in southern Britain, has varied over the past two millennia. Data are also available for various other regions of the world, notably north and meso America, Bulgaria, China, France, Japan, and Russia. Because it is a directional effect generated by currents in the fluid part of the core it is not surprizing that the patterns of variation are different between places more than a few thousand kilometres apart. Although these patterns and their relationships are of geophysical interest, from the dating point of view their localism is a disadvantage; it means that an essential prerequisite for archaeomagnetic dating is the establishment of reference values for the region concerned. Reference values are obtained using samples from pottery kilns and fireplaces of known age; lake sediments dated by radiocarbon are also used, as well as bricks and tiles in respect of inclination.

A basic drawback is there are repetitions of direction, both deinclination and inclination having the same value in two different periods—though such ambiguities can sometimes be resolved by also measuring palaeointensity. Nevertheless it proves to be a useful, but limited, technique and latterly systems have been developed to give assessment of the dating error limits taking into account the uncertainty of the reference dating as well as the uncertainty in measurement of the ancient direction (e.g. Batt 1997, Sternberg 1997). To minimize this latter uncertainty it is necessary to take about a dozen samples well distributed around the structure in order to average out distortion of the remanent direction by the magnetization of the baked clay itself and by settling-down movement subsequent to last cooling.

5.3. The polarity timescale

Much more dramatic than the minor perturbations comprising the secular variation are the complete reversals of the magnetic field, representing reversals of the direction of current flow in the dynamo system of the core. Major reversals occur roughly every million years but within the intervening periods—*chrons*—there are also *subchrons*—short periods of polarity opposite to that for most of the chron. The present chron—the *Brunhes*—began 780 000 years ago; it was preceded by the reversed-polarity *Matuyama* chron which began 2 500 000 years ago. Direct application to Palaeolithic sites is sometimes possible when a polarity change is recorded in associated sediment; figure 18 shows an example from a site in Spain where the reversed polarity found for the sediment containing hominid fossils indicates human arrival in Europe as long ago as at least around 800 000 years—contrary to strong contention by one school of thought that it was only 500 000.

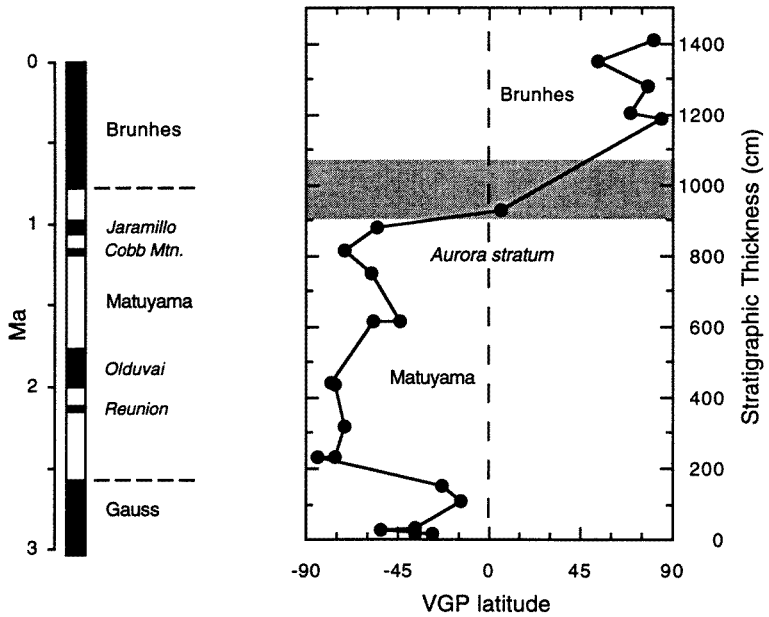

Figure 18. Magnetic pole (VGP) latitudes (shown on the right) that were obtained from sediment at the Atapuerca site in Spain (Parés and Pérez-Gonzalez 1995); hominid fossils were found in the Aurora stratum at 800 m. The VGP latitude refers to the virtual geographic pole representing the hypothetical dipole at the centre of the Earth that would give the observed angle of dip at the site. An extract from the polarity timescale is shown on the left, with blackened segments indicating normal polarity; four subchrons are indicated during the Matuyama chron but were not recorded in the sediment of the site, possibly because the sampling interval was too short. There are also subchrons (reversed) during the Brunhes chron but uranium-series dating higher in the section rules out association of the Aurora stratum with any of these (modified from Sternberg 1997).

6. Palaeoclimatology and astronomical dating

6.1. Manifestations of palaeoclimate

Long before the physical clocks intrinsic to a sample became technologically possible Palaeolithic chronology was substantially reliant on the placement of archaeological sites within a climatically determined framework. The parameters such as flora, fauna, soil conditions, and geomorphic units (e.g. glacial moraines) were, and are, used; an example is the changing spectrum of temperature-sensitive types of tree and shrub evidenced by pollen sequences in the vertical sections of archaeological sites; an interlocking dimension was, and is, the archaeological record of hominid development and technology. Currently being exploited are the rich archives of palaeoclimatic data contained in thick banks of sediment, notably in China and further north; during cold periods there is deposition of wind-blown loess and during intervening warmth there is the formation of organic-rich soil.

Climatic frameworks originated in the nineteenth century following geological recognition that there had been several successive periods of European alpine glacier advance and retreat; in the Alps the four recognised Ice Ages were named *Günz*, *Mindel*, *Riss*, and *Würm*, the latter being the more recent (in North America the corresponding glacial periods were named *Nebraskan*, *Kansan*, *Illinoian*, and *Wisconsinian*). In the terminology of NW Europe the Riss–Würm interglacial period is called the *Eemian* (the *Ipswichian* in the British Isles) and

the succeeding glaciation the *Weichselian* (the *Devensian* in the British Isles).

As research on archaeological and other sites intensified it became evident that the situation was more complex than major glaciations separated by interglacial periods: for instance, warmish, short-lived *interstadials* within glacial periods were recognized and with this increase in detail correlation between regions became less clear. As a result it became desirable to utilize the worldwide climatic framework provided by oxygen-isotope variations in deep-ocean sediment (see section 6.3) for which the timescale is now provided by astronomical dating (see section 6.2). Superimposed on the variations documented in these sediments there are more rapid fluctuations—as revealed by measurements on long vertical cores of ice from polar regions (see section 6.4); somewhat surprisingly there is increasing evidence that this ice-core record is representative of worldwide palaeoclimate.

Dendrochronology. Although this section is mainly concerned with climatic changes on a 1000-year basis it is convenient to include mention of the year-to-year variations that make possible the availability of wood, dendrochronologically dated to a high accuracy, for calibration of the radiocarbon timescale back to around 10 000 years ago. Many species of tree show recognizable annual rings and so the commencement date of a recently felled tree can be found by counting. Getting further back in time is possible because the width of a ring is influenced by climate and for some species the distinctive pattern of wide and narrow rings makes *cross-dating* possible between trees of a given region; in this technique the pattern of the inner rings of a recently felled tree is matched with the pattern of the outer rings of a 'fossil' tree whose life span just overlapped the younger tree; the overlapping is applied to successively older fossil trees and with great diligence the formation age of very old wood can be found—by a no more complex technique than counting. Long-lived trees with a life span of the order of 1000 years are at a premium for this process; also, considerable experience and expertise is needed to avoid error due to years in which the climate was so adverse that a ring is barely discernible, or, due to years in which the climate was such as to produce a double ring in the course of one year's growth. In some regions only a 'floating chronology' is obtained; this means that it has not been possible, at any rate initially, to link the records from fossil trees with that of a recent tree and anchoring by some means such as radiocarbon 'wiggle-matching' (section 2.1.4) is necessary in order to relate the rings to calendar dates (see, for instance, Kuniholm *et al* 1996).

Of course dendrochronology is important too in direct application to archaeological timbers. It also has a strong role in palaeoclimatology and indirectly, through climate-modification, as a recorder of major volcanic eruptions (see section 6.4).

6.2. The Milankovitch astronomical theory of climate

Speculation that the Ice Ages were triggered by variation in the amount, and distribution, of solar radiant energy falling on the Earth began in the mid nineteenth century and culminated in the work of the Yugoslav astronomer Milankovitch during the 1920s and 1930s, who published detailed insolation curves for the past 600 000 years. The variation is the result of small perturbations to the Earth's orbital motions caused by the changing configurations of the planets through their gravitational influences. The calculations of Milankovitch have subsequently been refined and extended further back in time (e.g. by Berger and Loutre 1991) The parameters of the motions concerned are:

(i) the eccentricity of the orbit around the sun (varying, due to perturbation, with periodicities of 100 000 and 413 000 years),

(ii) the obliquity, or tilt, of the ecliptic (varying with an average periodicity of about 41 000 years), and,

(iii) the precession of the equinoxes (varying with a mean periodicity of about 22 000 years).

With regard to (i), the present orbit is an ellipse of quite small eccentricity, the difference between furthest Earth–sun distance and nearest being 3%; over the past 200 000 years the difference has varied between near to 2 and 10%. The tilt (ii) is the angle between the equatorial plane of the Earth and the plane of its orbit; the present value is 23.4° and in the past it has varied between 21.8 and 24.4°. The precession of the equinoxes (iii) occurs because the Earth's axis of rotation wobbles in a similar manner to the axis of a spinning top (in itself this wobble does not involve a change in tilt); at present, midsummer in the Northern Hemisphere (i.e. the North Pole tilted towards the sun) occurs when the Earth is almost at that point in its elliptical orbit which is furthest away from the sun whereas approximately 11 000 years ago northern midsummer was occurring when the Earth was at its nearest point to the sun.

As far as the overall annual insolation is concerned it is only eccentricity variations that will have a direct effect, and that slight—hence use of the word 'triggering'; Milankovitch considered that when summer insolation in northern latitudes fell below a certain value a major glaciation was likely after a lag of some thousands of years. It was not until the mid 1960s that there began to be a general acceptance of the link between climate and perturbations in orbital motions. One reason for this was that uranium-series dating of raised coral beaches in Barbados and elsewhere (indicative of high sea levels and hence of minima in glacier volume) corresponded well with maxima in insolation. Another was that analysis of the growing body of deep-ocean climatic data (section 6.2) revealed the same periodicities, according to radiometric dating, as those of the orbital perturbations (for a highly readable account of the factors leading to acceptance of the link see Imbrie and Imbrie (1986)). Once the correlation was firmly established it became possible to use the astronomical data to give more accurate dating for the global climatic variations than was possible radiometrically; this is through the complex reiterative process of 'orbital tuning' (Imbrie *et al* 1984).

6.3. Oxygen-isotope variations in ocean sediments

As a result of temperature-dependent fractionation processes the ratio between the stable isotopes of oxygen is an indicator of climate. In glaciers, the ratio of around 0.002 of one of the minor isotopes, ^{18}O, to the principal isotope, ^{16}O, is slightly lower than that in sea water; the consequence is that during glacial times, because of the greater amount of water locked up in glaciers, sea water is isotopically heavier than during interglacial periods. Shells formed in this water are heavier still because there is a further fractionation during the formation of shell carbonate, lower temperature favouring incorporation of ^{18}O; however, in most regions, the dominant influence is glacier volume.

One of the first records of oxygen-isotope variation in deep-sea sediment was obtained by Emiliani (1955) who initiated the labelling system for successive warm and cold periods: odd numbers for the former and even for the latter. Samples are obtained by means of long coring tubes, of the order of 10 cm in diameter; the resulting stratigraphic column also carries a magnetic polarity record which allows direct location of the climatic variations on the polarity timescale (section 5.3). Figure 19 shows the variations found in a core of length 40 m; as will be seen the rate of sediment deposition is slow, being only a few millimetres per century; for many sediments the rate is slower and hence only boundaries between major reversals are then detectable. Essentially the same pattern is found in cores all around the world in agreement with the interpretation of the variations as primarily reflecting the amount of water locked up

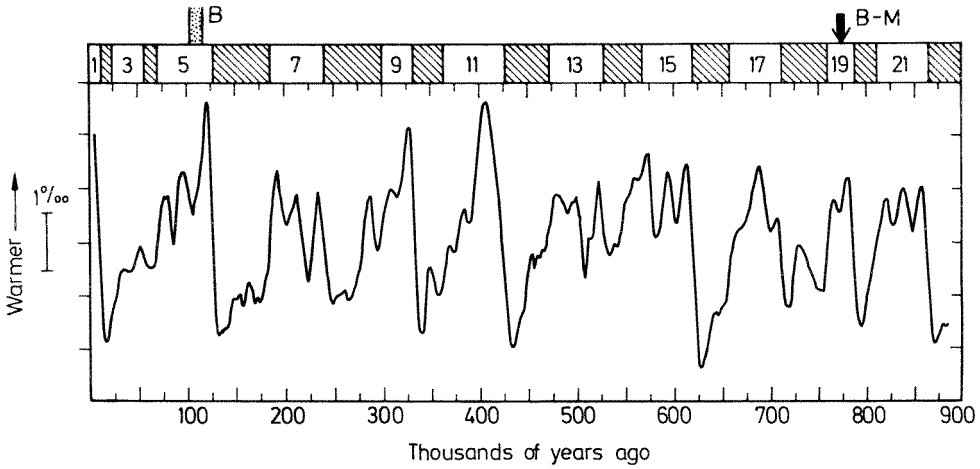

Figure 19. Oxygen-isotope variation in microfaunal remains from deep-ocean sediment (redrawn with additions, from Bassinot *et al* 1994). The vertical scale indicates the deviation of the isotope ratio from a standard, in parts per thousand. Along the top the numbers allocated by Emiliano (1955) to warm stages are given, with intervening cold stages being shown shaded. The Brunhes–Matuyama magnetic reversal is indicated by *B–M* and the Blake subchron by *B*. Using longer cores many earlier stages than are shown here have been identified. The timescale is astronomically based (from Aitken and Stokes 1997).

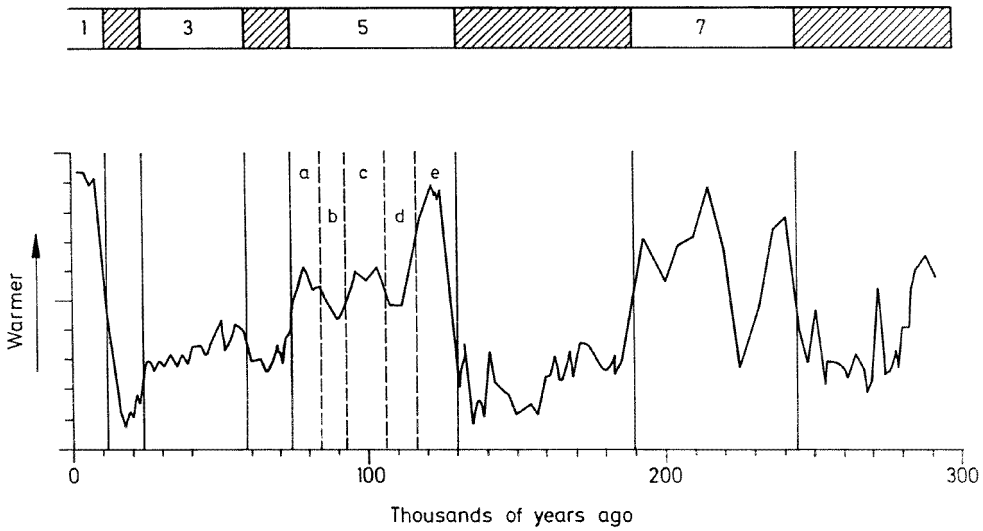

Figure 20. Oxygen-isotope variation for the past 300 000 years, with astronomically based timescale (redrawn, with additions, from Martinson 1987).The vertical axis represents the averaged ratio found in bottom-dwelling foraminifera from five locations in the oceans of the world: five divisions equals a change of one part per thousand. Warm stages are indicated along the top with intervening cold stages being shown shaded. The letters (*a*, *c*, *e*) refer to warm substages (from Aitken and Stokes 1997).

in the polar ice caps and glaciers—and hence worldwide climate; another manifestation of this locking-up is the fall in sea level by about a hundred metres during a glacial period.

Of particular archaeological interest in figure 19 is the peak occurring at the onset of warm

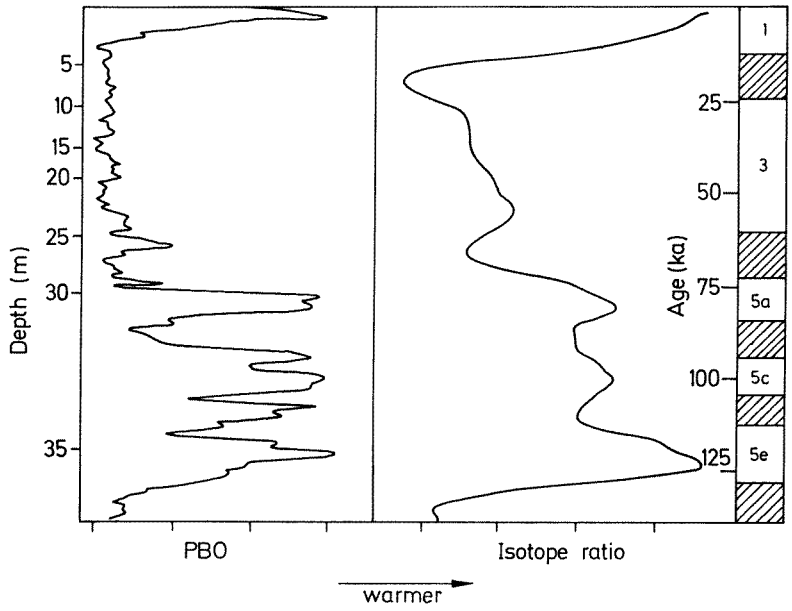

Figure 21. Comparison of the mid-latitude pollen record with deep-ocean oxygen-isotope variation. The curve on the left (redrawn, with additions, from Guiot *et al* 1989) is derived from analysis of pollen found in a peat bog at Les Echets, central France. The curve on the right is the SPECMAP version (Imbrie *et al* 1984) of the deep-ocean record, with astronomically based timescale and isotope stages indicated; each scale division corresponds to a change in ratio of one part per 1000. The pollen record is expressed in terms of the palaeobioclimatic operator (PBO), a more subtle indicator of temperate coditions than the percentage of tree pollen. Radiocarbon dating of the peat extended only to 30 000 years ago; earlier ages have been assigned on the basis of matching to the isotope variations and this accounts for the nonlinearity in the depth scale (from Aitken and Stokes 1997).

Stage 5 for which a comparable temperature to that of the present interglacial is indicated. The core of figure 20 shows this peak in more detail; of the successive warm substages it is 5e that is usually considered as the last interglacial period, representing the Riss–Würm interglacial in Alpine terminology and the Eemian in that of NW Europe.

Of course for archaeology and environmental studies the critical question is the extent to which the marine variations are representative of continental climate; a number of sites have long climatic records and these give a positive answer (see, for instance, Lowe and Walker 1997). Figure 21 shows an example and illustrates how the astronomical timescale can be transferred to land. Also, the succession of warm and cold stages is notably recognizable in the loess deposits of China and elsewhere (see, for instance, Kukla *et al* 1990, Forster and Heller 1994, Shackleton *et al* 1995, Zhou and Shackleton 1999).

There are other isotopes that can be used as climatic indicators; for instance, the ratio of stable isotopes of carbon, ^{13}C to ^{12}C, is used in precipitated carbonates in lake sediments and in stalagmitic carbonate in caves. Deuterium relative to light hydrogen is another indicative ratio and has been used for ice.

6.4. The climatic archive of polar ice

The build-up of polar ice involves the accumulation of snow, trapped air bubbles, and aerosolic components, e.g. dust, salt and volcanic ash. This archive is sampled by means of long cores

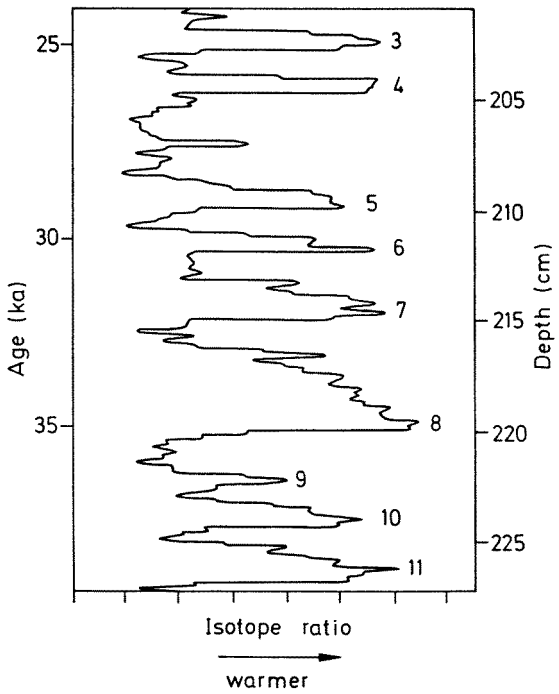

Figure 22. Part of the oxygen-isotope record from an Arctic ice-core—the continuous GRIP core drilled at Summit, Greenland (redrawn, with additions, from Dansgaard *et al* 1993); one division of the horizontal scale corresponds to a change of one part per 1000. The major warm peaks are termed *Dansgaard–Oeschger* events and represent interstadials occurring during the last glacial period. The pollen record also indicates warm periods within the last glaciation and from radiocarbon dating of these there is indication of correlation with the warmer peaks of the ice-core record.

drilled from the crests of the ice caps; in some cases the length totals more than 3 km and extends just beyond ice deposited in Substage 5e, the last interglacial. Because of temperature-dependent fractionation the oxygen-isotope ratio in the ice reflects the ambient air temperature at formation; the long-term pattern of variation follows the pattern found in ocean sediments but, because the accretion rate is much greater in the Arctic, shorter-term fluctuations are detectable there (such as shown in figure 22). In the upper part of an Arctic core annual layers are detectable because of seasonal variation of dust and acidity, allowing dating by counting back to about 15 000 years ago. Further down the layers become too thin for counting and estimates have to be made on the basis of models of glacier flow, ice movements, and accretion rates. Confirmation of the validity of these estimates is given by the agreement of the ages obtained for the main climatic phases with those of the ocean record (e.g. Bender *et al* 1994).

As will be seen in figure 22 the fluctuations in isotopic ratio are remarkably rapid, some lasting only for the order of a thousand years, with onset and termination sometimes being only a matter of decades. From the archaeological point of view the critical question is whether or not these fluctuations are representative of worldwide climate. The agreement, noted by Bender *et al* (1994), between a long core from the Arctic with one from the Antarctic is consistent with a positive answer, and increasingly, land-based evidence supports this too. Such evidence comes mainly from the climatic indications obtained from lake sediment and pollen sequences; there are also oxygen-isotope measurements on land molluscs and carbon-isotope measurements on cave carbonate that give strong endorsement. Hence although the situation is complex owing to the rapidity of the variations there is the eventual prospect that changes in the pollen spectrum on archaeological sites will be datable by reference to the ice-core record. It has been noted earlier (figure 20) that the major changes can be linked to the astronomical timescale.

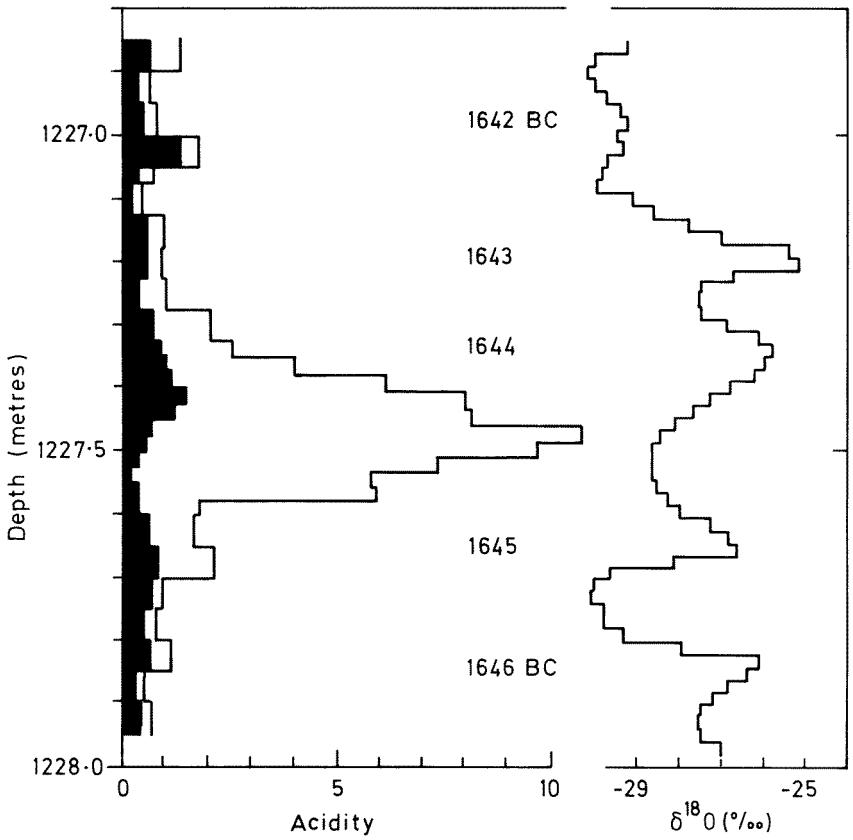

Figure 23. Part of the record from the Dye-3 ice-core, Greenland (redrawn from Hammer *et al* 1987).The filled histogram on the left represents nitric acid concentration and the unfilled histogram suphuric acid plus nitric acid; the strong peaking of sulphuric acid is indicative of a powerful volcanic eruption somewhere in the world, considered by the authors to be that of Thera. Oxygen-isotope values are shown on the right with calendar dates being shown in the middle; the rightward peaks correspond to summer (from Aitken 1990).

The Bronze Age eruption of Thera. As an illustration of the interlocking nature of chronological indications an outline is now given of the contentious and long drawn-out dating of the massive eruption, during Minoan times, of the volcano of Thera on the Aegean island of Santorini. Besides laying waste the advanced Bronze Age civilisation on that island—sometimes claimed to be the mythical Atlantis—there was also associated destruction on the island of Crete as well as ash fall on the island of Rhodes. Ice-core data is relevant because most volcanic eruptions inject huge amounts of dust and sulphur compounds into the atmosphere; the sulphuric acid aerosols resulting from the latter component cause there to be enhanced acidity in the snow deposited soon after an eruption and this is detectable in an ice core; figure 23 shows detail of an acidity peak proposed as being associated with the eruption of Thera and dated to 1644 (±20) BC (Hammer *et al* 1987).

The traditional archaeological chronology for the region, based on artefact and other links to the Egyptian calendar, places the event at around 1500 BC, well remote from the above date; however reassessment of the archaeological linkages has yielded a revised archaeological 'long' chronology concordant with it. This reassessment is unacceptable to traditionalists who,

apart from disagreement about the reassessment of the linkages, discount the ice-core evidence, pointing out that the peak could equally well refer to an eruption somewhere else around the world. The same criticism is made of climatic indications from tree-ring records; these are archives of volcanic activity because of the deleterious effect on worldwide climate through shielding of solar radiation by dust in the atmosphere, leading to abnormal annual growth rings in trees. Observation of frost-damaged growth rings in fossil bristlecone pines in California (La Marche and Hirschboeck 1984) as well as of severely attenuated growth in fossil bog oaks in Ireland (Baillie and Munro 1988) led to a date for the eruption of close to 1628 BC being put forward. An abnormal growth ring of about the same date has also been noted in the tree-ring chronology established for Turkey, much closer to the site of the eruption (Kuniholm *et al* 1996).

The long chronology also receives support from radiocarbon despite the period concerned being one in which the vagaries of the calibration curve leads to a wide range in calendar date for a precise radiocarbon age; nevertheless, as illustrated in figure 6, the results give a very low probability for a date of *circa* 1500 BC and are strongly supportive of the eruption being much earlier. Further, calendar dates obtained the archaeological period succeeding the one in question (Houseley *et al* 1999) are in direct conflict with the short archaeological chronology for that period, strongly favouring the long one and by implication an early date for the eruption.

Although this somewhat circumstantial evidence gives credence to the above ice-core and tree-ring data as being relevant to the eruption strong objections have been put forward against too-ready acceptance (e.g. Renfrew 1996, Buckland *et al* 1997); relevance to *some* eruption is not contested but it is argued that the probability of it being the one in question is low. There was expectation of resolution when, in another Greenland core, four minute specks of volcanic glass were found in the ice of an acidity peak that, within dating error limits, correlated with the ice-core and tree-ring indications already mentioned (Zielinski *et al* 1994). Comparison of the chemical composition of these specks and with that of glass from the eruption led Zielinski and Germani (1998a, b) to discount correlation; on the other hand the interpretation of Manning (1998) was diametrically opposite. The saga goes on.

7. Concluding remarks

One generalization that might be made is that the complexity of the execution is out of all proportion to the simplicity of the basic idea; fortunately this complexity reveals itself gradually—otherwise the prospect for pioneers of a method would be too daunting. Trial in application brings into focus unforeseen difficulties and the adage ‘the proof of the pudding is in the eating’ is highly relevant.

Complexity of execution often stems, in part at any rate, from the complexity of nature and laboratory physicists wishing to put their expertise to archaeological use need to seek cooperation from a range of Earth scientists (who also utilize these methods) quite apart from educating themselves in the archaeological problems concerned; an appreciation of the remarkable expertise of archaeologists is essential.

Acknowledgments

I am grateful to a number of colleagues who have helped me in the writing of this review and particularly to Grzegorz Adamiec and Liping Zhou.

References

Adamiec G and Aitken M J 1998 Dose-rate conversion factors: update *Ancient TL* **16** 37–50

Aitken M J 1985 *Thermoluminescence Dating* (London: Academic)

——1990 *Science-based Dating in Archaeology* (London: Longman)

——1998 *Introduction to Optical Dating* (Oxford: Oxford University Press)

Aitken M J and Stokes S 1997 Climatostratigraphy *Chronometric Dating in Archaeology* ed R E Taylor and M J Aitken (New York: Plenum)

Aitken M J, Stringer C B and Mellars P A (ed) 1993 *The Origin of Modern Humans and the Impact of Chronometric Dating* (Princeton, NJ: Princeton University Press)

Arnold J R and Libby W F 1949 Age determinations by radiocarbon content: checks with samples of known age *Science* **110** 678–80

Bada J L, Herrman B, Payan I L and Man E H 1989 Amino acid racemization in bone and the boiling of the German Emperor Lothar I *Appl. Geochem.* **4** 325–7

Bahn P G 1996 Further back down under *Nature* **383** 577–8

Bailiff I K 1993 Measurement of the stimulation spectrum (1.2–1.7 eV) for a specimen of potassium feldspar using a tuneable solid state laser *Radiat. Protection Dosimetry* **47** 649–53

——1997 Retrospective dosimetry with ceramics *Radiat. Meas.* **27** 923–41

Baillie M G L and Munro M A 1988 Irish tree rings, Santorini and volcanic dust veils *Nature* **332** 344–6

Bard E 1998 Geochemical and geophysical implications of the radiocarbon calibration *Geochimica Cosmochimica Acta* **62** 2025–38

Bard E, Hamelin B, Fairbanks R G and Zindler A 1990 Calibration of the ^{14}C timescale over the past 30 000 years using mass spectrometric U–Th ages from Barbados corals *Nature* **345** 405–10

Bard E, Raisbeck G, Yiou F and Jouzel J 1997 Solar modulation of cosmogenic nuclide production over the last millenium: comparison between ^{14}C and ^{10}Be records *Earth Planet. Sci. Lett.* **150** 453–62

Bassinot F C, Labeyrie L D, Vincent E, Quidelleur X, Shackleton N J and Lancelot Y 1994 The astronomical theory of climate and the age of the Brunhes-Matuyama magnetic reversal *Earth Planet. Sci. Lett.* **126** 91–108

Batt C M 1997 The British archaeomagnetic calibration curve: an objective treatment *Archaeometry* **39** 153–68

Bender M, Sowers T, Dickson M-L, Orchardo J, Grootes P, Mayewski P A and Meese D A 1994 Climate correlations between Greenland and Antarctica during the past 100 000 years *Nature* **372** 663–6

Berger A and Loutre M F 1991 Insolation values for the climate of the last 10 million years *Quat. Sci. Rev.* **10** 297–317

Berzero A, Caramella-Crespi V and Cavagna P 1997 Direct gamma-spectrometric dating of fossil bones: preliminary results *Archaeometry* **39** 189–203

Buckland P C, Dugmore A J and Edwards K J 1997 Bronze Age myths? Volcanic activity and human response in the Mediterranean and North Atlantic regions *Antiquity* **71** 581–93

Clark A J, Tarling D H and Noel M 1988 Developments in archaeomagnetic dating in Britain *J. Archaeological Sci.* **15** 645–68

Clark R J and Bailiff I K 1998 Fast time-resolved luminescence spectroscopy in some feldspars *Radiat. Meas.* **29** 553–60

Coote G E, Sparks R J and Blattner P 1982 Nuclear microprobe measurement of fluorine concentrations, with application to archaeology and geology *Nucl. Instrum. Methods* **197** 213–21

Dansgaard W *et al* 1993 Evidence for general instability of past climate from a 250-kyr ice-core record *Nature* **364** 218–20

Damon P E *et al* 1989 Radiocarbon dating of the Shroud of Turin *Nature* **337** 611–5

Duller G A T, Botter-Jensen L, Kohsiek P and Murray A S 1999 A high sensitivity optically stimulated luminescence scanning system for measurement of single sand-sized grains *Radiat. Prot. Dosim.* **84** 325–30

Emiliani C 1955 Pleistocene temperatures *J. Geology* **63** 538–78

Fleischer R L, Price P B, Walker R M and Leakey L S B 1965 Fission track dating of a mesolithic knife *Nature* **205** 1138

Forster Th and Heller F 1994 Loess deposits from the Tajik depression (central Asia): magnetic properties and paleoclimate *Earth Planet. Sci. Lett.* **128** 501–12

Fullagar R L K, Price D M and Head L M 1996 Early human occupation of northern Australia: archaeology and thermoluminescence dating of Jinmium rock-shelter, Northern Territory *Antiquity* **70** 751–73

Galbraith R F, Roberts R G, Laslett G M, Yoshida H and Olley J M 1999 Optical dating of single and multiple grains of quartz from Jinmium rock shelter, northern Australia. Part I: experimental design and statistical models *Archaeometry* **41** at press

Godfrey-Smith D I and Cada M 1996 IR stimulation spectroscopy of plagioclase and potassium feldspars and quartz *Radiat. Protection Dosimetry* **47** 379–85

Grün R 1997 Electron spin resonance dating *Chronometric Dating in Archaeology* ed R E Taylor and M J Aitken (New York: Plenum) pp 217–60

Guiot J, Pons A, de Beaulieu J L and Reille M 1989 A 140 000-year continental climate reconstruction from two European pollen records *Nature* **338** 309–13

Hammer C V, Clausen H B, Friedrich W L and Tauber H 1987 The Minoan eruption of Santorini in Greece dated to 1645 BC? *Nature* **328** 517–9

Hare P E, Von Endt D W and Kokis J E 1997 Protein and amino acid diagenesis dating *Chronometric Dating in Archaeology* ed R E Taylor and M J Aitken (New York: Plenum) pp 261–96

Houseley R, Hedges R E M, Law I A and Bronk C R 1990 Radiocarbon dating by AMS of the destruction of Akrotiri *Thera and the Aegean World III* ed D A Hardy (London: Thera Foundation) pp 207–15

Houseley R A, Manning S W, Cadogan G, Jones R E and Hedges R E M 1999 Radiocarbon, calibration, and the chronology of the late Minoan IB phase *J. Archaeological Sci.* **26** 159–71

Huntley D J, Godfrey-Smith D I and Thewalt M L W 1985 Optical dating of sediments *Nature* **313** 105–7

Hütt G, Jaek I and Tchonka J 1988 Optical dating: K-feldspars optical response stimulation spectra *Quat. Sci. Rev.* **7** 381–6

Ikeya M 1994 ESR (EPR) dating based on natural radiation effects *Nucl. Geophys.* **8** 201–24

Imbrie J and Imbrie J Z 1986 *Ice Ages* (Cambridge, MA: Harvard University Press)

Imbrie J, Hays J D, Martinson D G, McIntyre A, Mix A C, Morley J J, Pisias N G, Prell W L and Shackleton N J 1984 The orbital theory of Pleistocene climate: support from a revised chronology of the marine δ^{18}O record *Milankovitch and Climate, Part I* ed A Berger *et al* (Dordrecht: Reidel) pp 269–305

Kitagawa H and van der Plicht J 1998 Atmospheric radiocarbon calibration to 45 000 yr BP: Late Glacial fluctuations and cosmogenic isotope production *Science* **279** 1187–90

Kukla G, An A S, Melice J L, Gavin J and Xiao J L 1990 Magnetic suceptibility record of Chinese loess *Trans. R. Soc. Edinburgh: Earth Sci.* **81** 263–88

Kuniholm P I, Kromer B, Manning S W, Newton M, Latini C E and Bruce M J 1996 Anatolian tree rings and the absolute chronology of the eastern Mediterranean 2220–718 BC *Nature* **381** 780–3

Laj C, Mazaud A and Duplessey J-C 1996 Geomagnetic intensity and ^{14}C abundance in the atmosphere and ocean during the past 50 kyr *Geophys. Res. Lett.* **23** 2045–8

La Marche V C and Hirschboeck K K 1984 Frost tree rings in trees as records of major volcanic eruptions *Nature* **307** 7121–6

Lamothe M, Balescu S and Auclair M 1994 Natural IRSL intensities and apparent luminescence ages of single feldspar grains extracted from partially bleached sediments *Radiat. Meas.* **23** 555–62

Leach B F and Hamel G E 1984 The influence of archaeological soil temperatures on obsidian dating in New Zealand *New Zealand J. Sci.* **27** 399–408

Leach B F and Naylor H 1981 Dating New Zealand obsidians by resonant nuclear reactions *New Zealand J. Archaeology* **3** 39–49

Libby W F 1965 *Radiocarbon Dating* 2nd edn (Chicago: University of Chicago Press)

Libby W F, Anderson E C and Arnold J R 1949 Age determination by radiocarbon content: worldwide assay of natural radiocarbons *Science* **109** 227–8

Lowe J J and Walker M J C 1997 *Reconstructing Quaternary Environments* 2nd edn (New York: Longman)

Manning S W 1998 Correction. New GISP2 ice-core evidence supports 17th century BC date for Santorini (Minoan) eruption: response to Zielinski and Germani *J. Archaeological Sci.* **25** 279–89

——1998 Correction. New GISP2 ice-core evidence supports 17th century BC date for Santorini (Minoan) eruption: response to Zielinski and Germani *J. Archaeological Sci.* **25** 1039–42

Martinson D G, Pisias N G, Hays J D, Imbrie J, Moore T C and Shackleton N J 1987 Age dating and the orbital theory of the Ice Ages: development of a high-resolution 0 to 300 000-year chronostratigraphy *Quat. Res.* **27** 1–29

McDermott F, Grün R, Stringer C B and Hawkesworth C J 1993 Mass-spectrometric U-series dates for Israeli Neanderthal/early modern human sites *Nature* **363** 252–5

Mercier N, Valladas H and Valladas G 1995 Flint thermoluminescence dates from the CFR laboratory at Gif: contributions to the study of the chronology of the Middle Palaeolithic *Quat. Sci. Rev. (Quat. Geochronology)* **14** 351–64

Miller G H, Beaumont P B, Jull A J T and Johnson B 1992 Pleistocene geochronology and palaeothermometry from protein diagenesis in ostrich eggshells: implications for the evolution of modern humans *Phil. Trans. R. Soc.* B **337** 149–57

Miller G H, Magee J W, Johnson B J, Fogel M L, Spooner N A, McCulloch M T and Ayliffe L K 1999 Pleistocene extinction of Genyornis newtoni: human impact on Australian megafauna *Science* **283** 205–8

Murray A S and Roberts R G 1997 Determining the burial time of single grains of quartz using optically stimulated luminescence *Earth Planet. Sci. Lett.* **152** 163–80

Oakley K P 1955 Analytical methods of dating bones *Adv. Sci.* **11** 3–8
Parés J M and Pérez-Gonzalez 1995 Paleomagnetic age for hominid fossils at Atapeurca archaeological site, Spain *Science* **269** 830–2
Renfrew C 1996 Kings, tree rings and the Old World *Nature* **381** 733–4
Roberts R G 1997 Luminescence dating in archaeology: from origins to optical *Radiat. Meas.* **27** 819–92
Roberts R G *et al* 1998 Optical and radiocarbon dating at Jinmium rock shelter, northern Australia *Nature* **393** 358–62
Roberts R G, Galbraith R F, Olley J M, Yoshida H and Laslett G M 1999 Optical dating of single and multiple grains of quartz from Jinmium rock shelter, northern Australia part II: results and implications *Archaeometry* **41** at press
Schwarcz H P 1980 Absolute age determination of archaeological sites by uranium series dating of travertine *Archaeometry* **22** 3–25
——1992 Uranium series dating and the origin of modern man *Phil. Trans. R. Soc.* B **337** 131–7
——1997 Uranium series dating *Chronometric Dating in Archaeology* ed R E Taylor and M J Aitken (New York: Plenum) pp 159–82
Schwarcz H P, Simpson J J and Stringer C B 1998 Neanderthal skeleton from Tabun: U-series data by gamma spectrometry *J. Human Evolution* **35** 635–45
Shackleton N J, An Z, Dodonov A E, Gavin J, Kukla G J, Ranov A and Zhou L P 1995 Accumulation rate of loess in Tadjikistan and China and global ice volume *Quat. Proc.* **4** 1–6
Simpson J J and Grün R 1998 Non-destructive gamma spectrometric U-series dating *Quat. Geochronology* **17** 1009–22
Spooner N A 1998 Human occupation at Jinmium, northern Australia: 116 000 years ago or much less? *Antiquity* **72** 173–8
Sternberg R S 1997 Archaeomagnetic dating *Chronometric Dating in Archaeology* ed R E Taylor and M J Aitken (New York: Plenum) pp 323–56
Stuiver M and Becker B 1986 High precision calibration of the radiocarbon time scale, AD 1950–2500 BC *Radiocarbon* **28** 863–910
Stuiver M and Braziunas T F 1993 Sun, ocean, climate and atmospheric $^{14}CO_2$: an evaluation of causal and spectral relationships *The Holocene* **3** 289–305
Stuiver M and Kra R (ed) 1986 Calibration issue *Radiocarbon* **28** 805–1030
Stuiver M, Reimer P J and Braziunas T F 1998 High precision radiocarbon age calibration for terrestrial and marine samples *Radiocarbon* **40** 1127–51
Stuiver M and Pearson G W 1986 High precision calibration of the radiocarbon time scale, AD 1950–500 BC *Radiocarbon* **28** 805–38
Stuiver M, Pearson G W and Braziunas T F 1986 Radiocarbon calibration of marine samples back to 9000 Cal Yr BP *Radiocarbon* **28** 990–1021
Suess H E 1986 Secular variations of cosmogenic ^{14}C on Earth: their discovery and interpretation *Radiocarbon* **28** 259–65
Taylor R E 1987 *Radiocarbon Dating—an Archaeological Perspective* (Orlando: Academic)
Taylor R E and Aitken M J (ed) 1997 *Chronometric Dating in Archaeology* (New York: Plenum)
Visocekas R and Zink A 1999 Use of the far red TL emission of alkali feldspars for dosimetry *Quat. Sci. Rev.* **18** 271–8
Voelker A H L, Sarnthein M, Grootes P M, Erlenkeuser H, Laj C, Mazaud A, Nadeau M-J and Schleicher M 1998 Correlation of marine ^{14}C ages from the Nordic Seas with the GISP2 isotope record: implications for ^{14}C calibration before 25 ka BP *Radiocarbon* **40** 517–34
Walter R C 1997 Potassium–argon/argon–argon dating methods *Chronometric Dating in Archaeology* ed R E Taylor and M J Aitken (New York: Plenum) pp 97–126
Walton D, Share J, Rolph T C and Shaw J 1993 Microwave magnetisation *Geophys. Res. Lett.* **20** 109–11
Westgate J A, Sandhu A and Shane P 1997 Fission-track dating *Chronometric Dating in Archaeology* ed R E Taylor and M J Aitken (New York: Plenum)
Westgate J A, Shane P A R, Pearce N J G, Perkins W T, Korisettar R, Chesner C A, Williams M A J and Acharyya S K 1998 All Toba tephra occurrences across peninsular India belong to the 75 000 yr eruption *Quat. Res.* **50** 107–12
Wintle A G 1973 Anomalous fading of thermoluminescence in mineral samples *Nature* **245** 143–4
——1996 Archaeologically-relevant dating techniques for the next century *J. Archaeological Sci.* **23** 123–38
——(ed) 1997 Luminescence and ESR dating and allied research *Radiat. Meas.* **27** 625–1025
Yokoyama Y and Nguyen H-V 1981 Datation direct de l'Homme de Tautavel par la spectrometrie gamma, non destructive, du crâne humain fossile Arago XXI *Comptes Rendus des Sceances de l'Acadamie des Sciences, Paris, Serie III* **292** 741–4
Zhou L P and Shackleton N J 1999 Misleading positions of geomagnetic reversal boundaries in Eurasian loess and implications for correlation between continental and marine sedimentary sequencies *Earth Planet. Sci. Lett.*

168 117–30

Zielinski G A and Germani M S 1998a New ice-core evidence challenges the 1620s BC age for the Santorini (Minoan) eruption *J. Archaeological Sci.* **25** 279–89

——1998b Reply to: Correction. New GISP2 ice-core evidence supports 17th century BC date for Santorini (Minoan) eruption *J. Archaeological Sci.* **25** 1043–5

Zielinski G A, Mayewski P A, Meeker L D, Whitlow S, Twickler M S, Morrison M, Meese D, Alley R B and Gow A J 1994 Record of volcanism since 7000 BC from the GISP2 Greenland ice core and implications for the volcano-climate system *Science* **264** 948–52